

QGAIC: Quantum Inspired Genetic Algorithm for Image Classification

Akhilesh Kumar Singh^a, Kirankumar R. Hiremath^b

Email: akhileshkumarsinghse@gmail.com^a

Quantum Technology (IDRP), IIT Jodhpur, India^a, Department of Math, IIT Jodhpur, India^b

Abstract

This study uses two meta-heuristics methodologies to introduce two novel quantum-inspired meta-heuristic approaches: quantum-inspired genetic algorithm (QIGA1) and quantum-inspired genetic algorithm with dynamic approach (QIGA2). The two suggested methods combine a classical and quantum genetic algorithm approach. Both approaches use The correlation coefficient as an assessment function to identify the best (optimal) values for binary image. In quantum computing, they use simple ideas like qubits and state superposition. Due to these characteristics, parallelism—which uses the time discreteness of quantum mechanical systems—is exhibited. For five distinct MNIST datasets, the performance of all participating algorithms has been assessed by comparing the suggested approaches first with their traditional approach counterparts and then with the proposed methods QIGA1 and QIGA-2. Each method's ideal threshold value, associated fitness value (best and average), loss, and accuracy for each MNIST dataset have all been published. The outcomes demonstrate the superior efficiency of the suggested approaches over their traditional equivalents.

Keywords- Genetic Algorithm (GA), Quantum Genetic Algorithm (QGA), Quantum Inspired Genetic Algorithm (QIGA), Quantum Mutation (QM), Quantum Crossover (QC)

1. Introduction

A genetic algorithm (GAs) is a metaheuristic based on natural selection belonging to the broader evolutionary algorithms (EA) class. GAs are evolutionary algorithms based on Darwinian natural selection. Heuristic optimization techniques are widely utilized and grounded in simulated genetic processes, including mutation and crossover, and population dynamics, such as reproduction and selection (Zhou et al., 2006 and Beltra, 2016). Solutions are represented in multi-arrays known as chromosomes. The GA based-algorithm typically initiates with a randomly generated starting population of chromosomes and iteratively evolves this population in pursuit of an best solution. The limitation of these strategies is their dependence on sufficient data to train the model and enhance forecast accuracy. This constraint is consistent with the need for more precise and enough data in picture categorization. Quantum computing emphasizes advancing computational technology grounded in the principles of quantum theory. The QGA process results from integrating quantum computation and GAs, representing a novel probabilistic evolutionary process (Wang et al., 2010). In 1996, Narayanan and Moore originally suggested the quantum genetic method, successfully employed to resolve the real-life problem (TSP). QGA is fundamentally a variant of GA and can be utilized in any domain where traditional GAs is applicable. The efficacy of QGA markedly surpasses that of the traditional GAs. The QGA exhibits a limited population size, rapid convergence rate,

significant global optimization capabilities, and commendable robustness. The quantum state vector (QSV) is utilized in the GA to represent genetic programming, while quantum logic gates facilitate chromosome evolution.

Consequently, superior outcomes are attained. Nonetheless, standard QGA (Zhou et al., 2006 and Han et al., 2000) still presents specific issues. For instance, ascertaining the orientation of the quantum rotation angle depends on a reference table (rotation angle table-2). It results in a program with several evaluative criteria. Furthermore, the fixed rotational angle adversely affects rapid searching and subsequent convergence (Yang et al., 2004 and Huang et al., 2006). This study enhances the QGA with an adaptive evolution approach to address the issue above. quantum mutation, quantum population initialization, quantum fitness, and quantum crossover process are implemented to improve the algorithm's performance. Quantum computation contrasts with traditional computation. It employs superposition, coherence, and entanglement of various qubits in a quantum state to facilitate quantum computation (Yang et al., 2004 and Proakis, 2000). Quantum computation results from using quantum computation and mechanics in the realm of algorithms. The capacity for parallelism is the fundamental distinction between classical (traditional) and quantum computations. In the probability (amplitudes) calculation, the network (device) is not in a constant condition. Conversely, it possesses a specific probability, and the probability of QSV corresponds to many potential states. Quantum processing utilizes the probability of amplitudes of given states (i.e. quantum states), which are squared and normalized. Consequently, the computational power of quantum systems is \sqrt{N} times superior to that of classical computation. Quantum rotating gates achieve quantum transformation. Quantum computation possesses distinct features in comparison to classical computation (Wang et al., 2010, Beltra, 2016, and Han, 2002). Specific processes of these qualities can be integrated into optimization algorithms to enhance traditional optimization methods. Quantum computers utilize quantum bits, or qubits, which handle information fundamentally distinctly. Classical bits consistently represent either one or zero, but Quantum Inspired Genetic Algorithms (QIGA) present an innovative feature selection method to enhance their efficiency and efficacy in optimization problems. This work examines the three fundamental components of QIGA: qubit population representation, quantum rotation gate functionality, and crossover and mutation function for quantum populations. Integrating the GA with the superposition technique can significantly enhance image classification precision. Furthermore, the findings indicate that QIGA exhibits much greater efficiency than Classic GA. This advancement is attributable to QIGA's ability to achieve a more precise classification by applying the superposition principle inherent in quantum computing. Integrating the quantum tenets into evolutionary algorithms represents significant progress in feature selection methodologies. QIGAs possess the potential to revolutionize healthcare diagnostics and enhance patient outcomes and classification jobs across various domains, including healthcare and treatment.

This work aims to build an algorithm capable of independently evolving dynamic quantum genetic networks for image classification, overcoming the constraints of the current conventional genetic approaches discussed here. The concept of the binary flow-diagram of QIGA programming is presented in this research to encode the structural architectures of

quantum images in view of the outstanding performance measurement of quantum genetic programming in several real-life based applications. This paper makes primarily the following objectives:

1. Propose a novel QIGA with a dynamic feature selection and extraction technique and choose the appropriate environment selection for image classification to improve traditional classification strategies.
2. A meta-heuristic quantum inspired genetic programming with a dynamic model is proposed where the remote archive of non-dominated and optimal solutions and the best population achieved by a dynamic genetic quantum algorithm with quantum rotation gate with their adaptive adjustment theorems (1-2) and lookup tables-2. This approach helps prevent the algorithm from becoming caught in a local optimum and accelerates the convergence.
3. Five MNIST benchmark datasets frequently used in picture classification tasks and a real-life dataset prove the proposed method's efficacy—the suggested method's better performance over other state-of-computational findings demonstrates the-art methods.

The present paper has the following general framework: We discuss in Section-I Introduction, Section-II literature surveys of quantum-inspired genetic algorithms with image classification and MNIST based on genetic algorithms. Section-III provides a background to quantum computing and the foundations of conventional genetic algorithms, a comparison between GA and QGA, theory-linked quantum, gate-based quantum computation, and quantum image processing. Section-IV addresses architecture and its application to the MNIST dataset as a benchmark and the suggested quantum-inspired genetic algorithm (QIGA 1 and 2). Section-V presents the outcomes gained using the architecture on several kinds of datasets and conclusion.

2. Literature Review

The utilization of Quantum-inspired Genetic Algorithms (QIGAs) in picture classification has emerged as a significant study domain owing to their capacity to augment optimization methods and elevate model efficacy across diverse fields. Numerous studies have investigated how QGAs can enhance feature selection, augment classifier performance, and expedite convergence in image recognition tasks. This literature review analyses the contributions of several scholars in employing QGA for different picture classification issues, emphasizing both the benefits and drawbacks of their methodologies. Several academic writers are working on quantum QGAs, and their use in picture classification has aided the study, which uses the MNIST dataset. Each author has made substantial advances by combining quantum physics with classical approaches, increasing efficiency, accuracy, and computational performance.

Zhang et al. (2014) offer an improved QIGA for picture registration, an important step in image categorization. The technique provides adaptive rotation angle adjustment and a cooperative learning approach to improve convergence speed and solution quality. Experiments show that the modified QIGA beats traditional algorithms in accuracy and resilience. Phalak et al. (2024) researched using GAs to enhance quantum embeddings

for machine learning applications. Their research demonstrated the advantages of quantum embedding-based selection, notably in increasing the performance of quantum models on picture datasets such as MNIST and Tiny ImageNet. They demonstrated how GAs may systematically investigate and improve quantum embedding structures, resulting in higher model accuracy. Ranga et al. (2024) demonstrated a study of hybrid quantum neural networks that used parallel quantum circuitry. Their technique produced exceptional accuracy on the MNIST dataset, outperforming previous quantum-classical algorithms. They also tested their method on more complicated datasets, such as CIFAR-10, confirming the generality and effectiveness of quantum-enhanced layers for detecting and categorizing pictures based on shared traits. Riaz et al. (2023) developed neural network models using QGAs. Their study findings showed advances in multi-class image classification for benchmarking datasets. (i.e. CIFAR 10 and MNIST). They demonstrated how quantum processes might improve weight selection, feature extraction, and convergence in neural network designs, resulting in greater accuracy and performance. Senokosov et al. (2024) demonstrated that the quantum Hamiltonian embedding approach is used for image classification and reduces error with the help of quantum machine learning (QML). Their novel embedding approach enabled efficient encoding of picture data in quantum circuits, significantly improving the performance of data reuploading models. Their research demonstrated realistic quantum implementation on benchmark datasets such as digits-MNIST, sign-MNIST, and Fashion-MNIST, offering valuable insights into the quantum encoding process. Iordanis et al. (2020) contributed substantially by combining slow feature analysis (SFA) with quantum genetic classification approaches. Their technique lowered dimensionality while retaining good accuracy on datasets such as MNIST. Their quantum classifier performed well, demonstrating the power of integrating conventional feature extraction approaches with quantum principles to tackle real-world picture classification problems.

Table 1 shows the authors' work, highlighting the broad and potential uses QIGAs in image categorization. These researchers proved QIGA's efficacy in improving various model parameters and emphasized its potential in machine learning and computer vision applications. QIGA has shown to be a valuable tool in image classification, optimizing hyperparameters for CNNs, QNNs, and SVMs and improving feature selection, data augmentation, picture segmentation, and even generative models such as GANs.

Authors	Datasets	Advantage	Limitation	Contribution
Phalak et al. 2024	MNIST and Tiny ImageNet	Improved accuracy and reduced runtime compared to random feature-to-qubit mappings.	Limited to specific quantum embedding techniques and small datasets for demonstration.	Used optimizing quantum embeddings. Compared performance with Quantum Embedding Kernel (QEK), QAOA-based embedding and QRAC

Lentzas et al. 2019	MNIST, CIFAR-10	Faster and more efficient hyperparameter optimization compared to classical algorithms.	Focused mainly on hyperparameter ; no detailed comparison with advanced classical algorithms.	Explored QGA for hyperparameter tuning in machine learning. Demonstrated its potential in enhancing hyperparameter optimization classifiers.
Iordanis et al. 2018	MNIST	High accuracy (98.5%) with polylogarithmic runtime in data dimensions and size.	Dependency on quantum hardware for scalability.	Proposed a quantum classifier combining dimensionality reduction, classification with efficiency and accuracy, comparable with classical classifiers.
Choe et al. 2023	MNIST	Enhanced training efficiency and accuracy in quantum neural networks using QGA.	Requires quantum hardware for implementation; scalability concerns for larger datasets.	Introduced a quantum backpropagation model optimized with QGA, suggesting the potential of QGA in quantum neural network training.
Sophie Choe 2022	MNIST	Demonstrated the use of continuous variable quantum neural networks for MNIST classification.	Limited to small-scale experiments; practical implementation challenges on current quantum hardware.	Presented a hybrid classical-QNN model using continuous variable quantum circuits, showcasing the potential of QNNs in image classification tasks.
Kevin et al. 2024	Fashion-MNIST	Provided a proof of concept for quantum classification on real quantum hardware.	Achieved moderate accuracies; limited by current quantum hardware capabilities.	Implemented a variational quantum classifier using IBM's quantum computer. Demonstrated the feasibility of QML algorithms on standard datasets.
Creevey et al. 2023	Synthetic datasets	Developed a GA for preparing quantum states, generating low-depth quantum circuits for initialization.	Focused on state preparation; did not directly address optimization tasks like classification.	Introduced GASP, a GA designed to generate efficient quantum circuits for preparation of states, beneficial for initializing QML algorithms.
Senokosov et al. 2023	MNIST, CIFAR-10	Improved accuracy, quantum advantage in optimization tasks	Hardware limitations for practical deployment	Developed hybrid -QNN incorporating QIGA
Alisson Steffens et al. 2021	Fashion-MNIST	Reduced dimensionality, improved feature extraction	Limited adaptability to non-image datasets	Demonstrated QIGA's utility with feature selection and feature extraction.

Ranga et al. 2024	MNIST	Combines quantum computing with CNN. Demonstrates effectiveness in high-dimensional classification	Focuses on binary classification. extension to multi-class classification requires further research.	Presents a novel HQNN for image classification is Combined classical computing with quantum computing to enhance performance.
Zhang et al. 2022	Iris and MNIST	Proposes a robust training scheme for QNNs using a GA. Enhances accuracy distribution, leading to more reliable model performance	The impact of hyper-parameters is more evident on datasets; effects on other datasets may vary. validation on diverse datasets is necessary to confirm generalizability.	Develops a generalized training scheme incorporating GA to improve the robustness of quantum neural networks. Validates the approach showing. Contributes to the development of more reliable quantum neural network training methodologies.
Riaz et al. 2023	MNIST and CIFAR-10	Proposes a QGA-based neural network model for multi-class image classification. Demonstrates the potential of QGA in enhancing neural network performance.	Accuracy improvements are modest, indicating room for further optimization. performance on more complex datasets and real-world applications.	Develops a neural network model incorporating QGA for multi-class image classification. Contributes to the exploration of QGA in enhancing neural network models for image classification.
Soumyadip Sarkar 2024	Digits-MNIST	Integrates quantum computing with classical ML and Explores the potential of hybrid models in improving classification accuracy.	The reported accuracy is currently lower than that of purely classical models. Used optimization and advanced GA for achieving best performance.	Proposes a hybrid quantum-classical approach. Utilizes quantum circuits in conjunction with CNNs. Highlights the potential and challenges of integrating quantum computing in image classification tasks.
Mohsen et al. 2021	MNIST	Introduces a novel encoding mechanism for classification of larger and realistic images using quantum systems and comparable with CNN.	The approach requires further optimization for superior performance. Implementation is constrained by current quantum hardware limitations.	Proposes a framework for compression and classification using quantum deep learning. Demonstrates the feasibility of QML on classical datasets.

Table 1: Summary of Literature Survey

3. Background

This section will briefly recap some fundamentals of GA and terminology, which will help us understand our proposed model's basic concept introduced in section 3.

3.1 Conventional Genetic Algorithm (GA)

GAs are meta-heuristic optimization techniques that integrate several methodologies and notions derived from biological Darwinian development. These are algorithms derived from natural phenomena designed to address various issues across numerous areas. A GA consists of several fundamental components, as shown in Figure 1 and described in the sub-section below. An individual represents a singular solution. An individual may possess multiple attributes, yet it can be seen as a representation or encoding of a singular solution to the problem. A GA comprises a population that consists of several people. It may be seen as a compilation of individuals.

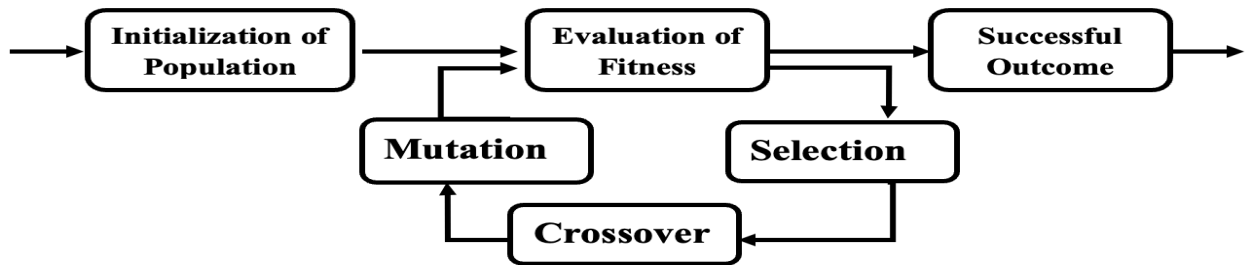


Figure 1: Overview of conventional genetic algorithm

3.2 Preliminaries

Qubits: In classical computing, the fundamental unit of information is the bit, which can denote either 0 or 1. In quantum computing, the essential unit is the qubit, which can represent $|0\rangle$ and $|1\rangle$. Vectors are represent by-

$$|0\rangle = \begin{bmatrix} 1 \\ 0 \end{bmatrix} \quad |1\rangle = \begin{bmatrix} 0 \\ 1 \end{bmatrix} \quad [1]$$

Pauli Dirac introduced these notation and called *ket* and *bra* for qubits representation.

Quantum Superposition (QS): Superposition is a crucial property of quantum physics, permitting qubits to exist in numerous states concurrently. A traditional bit can be either 0 or 1, whereas a qubit can exist in a superposition of both states, representing both 0 and 1 simultaneously until measured. A linear combination of vectors can represent QS. Considers two vectors $|0\rangle$ and $|1\rangle$ and represent in quantum superposition-

$$|\psi\rangle = \alpha |0\rangle + \beta |1\rangle \quad [2]$$

Where α and β are complex numbers and should satisfy this equation-

$$|\alpha|^2 + |\beta|^2 = 1 \quad [3]$$

Here, $|\alpha|^2$ and $|\beta|^2$ are amplitudes or probability of measuring both vectors state $|0\rangle$ and $|1\rangle$.

Theorem 1: Let consider a determinant $D = \begin{vmatrix} \alpha_i & \alpha_j \\ \beta_i & \beta_j \end{vmatrix}$. Where (α_i, β_i) is represents the probability or amplitudes of some vector states with known optimal solutions. (α_j, β_j) is represents vector state's probability of finding the optimal solution.

$$f(x_i) \neq f(b_i) = \begin{cases} D \neq 0, & \text{direction of the rotation angle will be negative.} \\ D = 0, & \text{direction of the rotation angle will be either positive or negative or both} \end{cases}$$

Proof: Let consider two state vectors are $|0\rangle$ and $|1\rangle$. There are two probabilities are- $[\alpha_i, \beta_i]^T$ and $[\alpha_j, \beta_j]^T$. The first probability is known optimal solution, and second probability is unknown state to find a solution. Let angle of both probabilities is represented by θ_i and θ_j , respectively.

$$D = \begin{bmatrix} \cos \theta_i & \cos \theta_j \\ \sin \theta_i & \sin \theta_j \end{bmatrix}$$

Case 1:

$$\text{If } D \neq 0 \begin{cases} 0 < \text{Mod}(\theta_j - \theta_i), & \text{direction of angle will be negative} \\ \pi < \text{Mod}(\theta_j - \theta_i) < 2\pi, & \text{direction of angle will be positive} \end{cases}$$

Case 2:

$$\text{If } D = 0 \quad \left\{ \text{Mod}(\theta_j - \theta_i) < 0 \text{ or } \pi, \text{ direction of rotation will be positive or negative or both} \right.$$

Theorem 2: The i^{th} bit of best member of previous generation value 'b' and chromosome 'x' are equal or not and fitness of b and x is also equal or not. Which is depend upon the rotation state. The rotation is calculated by transferring of b_i and x_i to b_{i+1} and x_{i+1} .

$$f(x_i) \neq f(b_i) = \begin{cases} x \neq b, & \text{True or False (Positive or Negative)} \\ x = b, & \text{True or False (Positive or Negative)} \end{cases}$$

Proof: Let we calculate best fit of previous member and chromosomes $f(b)_i$ and $f(x)_i$ on basis of change rotation of x and b.

Case 1: If $f(b)_i \neq f(x)_i$ and $[(b_i = 1, x_i = 0) \rightarrow (b_i = 0, x_i = 1)]$ then

$$\Delta\theta_i = \begin{cases} (\frac{\pi}{2} - \theta_i) * C_0 \\ -\theta_i * C_0 \end{cases}$$

Case 2: If $f(b)_i = f(x)_i$ and $[(b_i = 0, x_i = 1) \rightarrow (b_i = 0, x_i = 0)]$ then

$$\Delta\theta_i = \begin{cases} (\frac{\pi}{2} - \theta_i) * C_0 \\ -\theta_i * C_0 \end{cases}$$

Case 3: if $f(b)_i$ and $f(x)_i$ may be fit or not say and $[(b_i \text{ and } x_i \text{ are same}) \rightarrow (b_i \text{ and } x_i \text{ are opposite})]$ then

$$\Delta\theta_i = \begin{cases} (\frac{\pi}{2} - \theta_i) * C_0 \\ -\theta_i * C_0 \end{cases}$$

where C_0 is varying between -1 to +1.

3.3 Chromosomes- The quantum chromosome can be defined as

$$|\emptyset\rangle = a|x\rangle + b|y\rangle \quad [4]$$

Where the vectors x and y are representing lower and upper bound. Qubits are representing in superposition. Then the chromosomes can be representing by qubit:

$$\omega_i^p = \begin{bmatrix} a_{i,11}^p & a_{i,12}^p & a_{i,21}^p & a_{i,22}^p & \dots & a_{i,n-1}^p & a_{i,n}^p \\ b_{i,11}^p & b_{i,12}^p & b_{i,21}^p & b_{i,22}^p & \dots & b_{i,n-1}^p & b_{i,n}^p \end{bmatrix} \quad [5]$$

The size of chromosomes is n and evaluated with generating random number ($r_{i,j} \in [0,1]$) for qubits are $[a_{i,j}^p, b_{i,j}^p]^P$, $j \in \{1,2\}$. The chromosomes qubits are collapse in these two states and generate new states of chromosomes. The population size is P , and the initialization of population by randomly.

3.3.1 Structure and Measurement of Quantum Chromosomes- A Quantum Chromosome is a sequence of m qubits stored in a quantum register; alternatively, it can be described as constituting a quantum register of n bits. Figure 2 illustrates the architecture of a quantum chromosome.

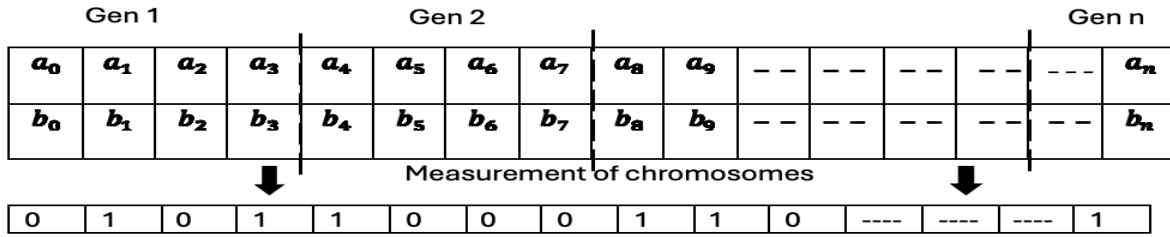


Figure 2: Sample of measurement of chromosomes

The measurement process initiates with chromosomes of minimal length for each dimension. Subsequently, at each stage, the size of the chromosomes expands by the magnitude of the interval until it attains its maximum height at the final level. The quantity of accuracy levels is determined by below equation.

$$Level_{Max} = \frac{\{Length_{Max} - Length_{Min}\}}{Interval} + 1 \quad [6]$$

4. Methodology

This section presents our suggested combination of quantum computing techniques and classical GA. In particular, we develop a quantum-inspired genetic algorithm (QIGA) by partially converting a conventional GA into a quantum one.

4.1 Proposed Model

QIGA demonstrates effective problem-solving capabilities in specific contexts; however, it is hindered by local stagnation and excessive reliance on initial parameters. However, it can continue to yield high-quality responses through enhancements and collaboration with

alternative methods. We present an enhanced QIGA1 algorithm optimized through the dynamic design of QIGA2. Figure 3 illustrates the proposed algorithm utilized for addressing a function approximation problem. This algorithm integrates GA with a Quantum approach, as the global search capability of QIGA2 enhances the convergence speed and accuracy of QIGA1. Various combination methods exist; however, we have selected to combine GA and Quantum techniques individually. This is due to our desire to quantify the extent of improvement that GA can provide for the QIGA algorithm. This method facilitates the assessment of GA's contribution to the QIGA algorithm. The proposed algorithm (QIGA) consists of three primary steps: QGA, environment selection, and feature selection and extraction utilizing GA.

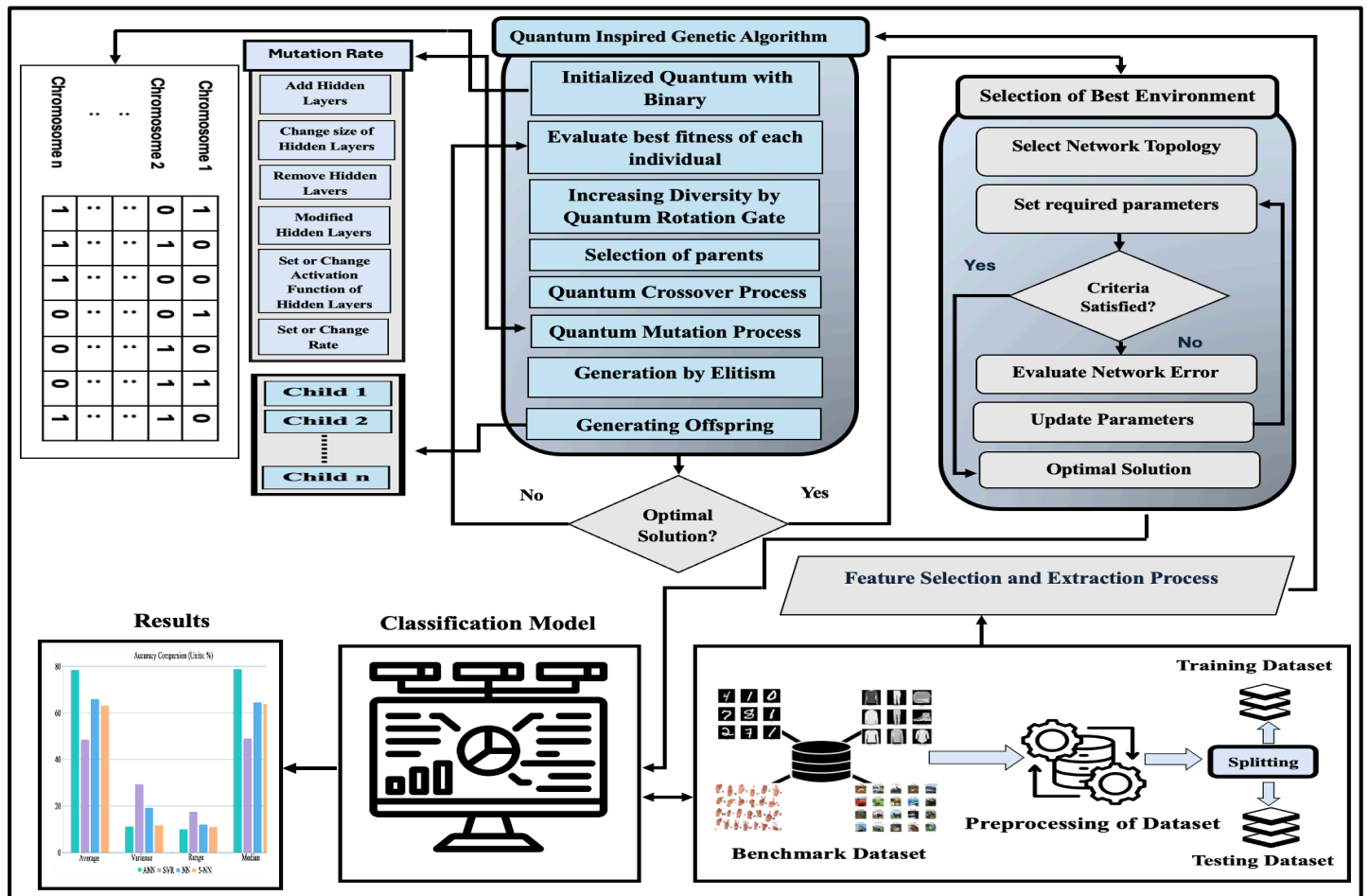


Figure 3: Proposed General Model for Quantum Inspired Genetic Algorithm (QIGA)

During the QGA step, the optimized variables are incorporated into the network as initial parameters and specific conditions must be satisfied to conclude the QGA process. This study employed optimal fitness and maximum iteration number as termination criteria. The most compelling aspect of this article is about to be revealed. In contrast to most prior studies, this research presents a novel methodology for comparing QIGA1 and QIGA2. This study is novel because previous research has not compared QIGA1 and QIGA2; instead, it has only compared QIGA1 with the enhanced version of QIGA1 that incorporates QGA. QIGA1 could enhance QIGA2, as the latter has overlooked the precise timing and other devotions associated with QIGA.

Furthermore, it is possible to ascertain whether a GA-combined Quantum algorithm would outperform the pure QIGA algorithm when provided with identical training time and relevant parameters. The rationale for employing distinct and separate QIGA1 and QIGA2 steps is now evident. The tasks outlined in the subsequent subsections are combined to form the suggested QIGA and demonstrated in figure 3. Quantum Computation's ideas have been incorporated into the well-known evolutionary algorithm known as the GA to create a quantum-inspired genetic algorithm (QIGA).

4.2 Proposed Algorithm

This article proposes two novel quantum-inspired meta-heuristic algorithms: the quantum-inspired genetic algorithm (QIGA1) and the quantum-inspired genetic algorithm with dynamic (QIGA2). The pseudocode of QIGA1 and QIGA2 are explain in algorithm 1 and 2. Figure 3 is a description of the general framework of these suggested approaches.

The Quantum-Inspired Genetic Algorithm (QIGA1) is an optimization technique that combines quantum ideas with conventional GA. The evolutionary process starts with initializing a quantum population, P_0 , using binary image representation (Algorithm 3). Equation 10 specifies the number of generations that the algorithm will go through. In each generation, individuals' fitness is assessed using Algorithm 4, and selection (Algorithm 6) is used to designate people for the next stage depending on their fitness. Quantum rotation gates are used to update the population P_0 , as per Algorithm 5 and Tables 2.

If certain conditions are met, quantum crossover (Algorithm 7) mixes characteristics from parent individuals to produce offspring. Quantum mutation (Algorithm 8) is then applied to offspring, adding variety while preventing premature convergence. These procedures are done on all people to increase variety and comprehensively investigate the solution space.

Following these modifications, the population's fitness is re-evaluated and ranked using Algorithm 4. The top-performing individual is preserved via the elitism process (Algorithm 9), ensuring the best solutions are preserved. Furthermore, the ideal environment matching the best individual is identified using an algorithm 11. The procedure repeats until the maximum number of generations is achieved. The program then generates the best person and environment-specific optimum solution. QIGA1 improves the flexibility and efficiency of classic GA by utilizing quantum-inspired approaches like rotation gates, crossover, and mutation.

```
// Algorithm 1: Quantum Inspired Genetic Algorithm (QIGA1) //
Input: Size of population P
Output: Best individual with best environment
1.  $P_0 = \emptyset$ 
2.  $P_0 =$  Initialization quantum population with binary image (using algorithm 3)
3. for  $i = 1$  to  $\max\_size\_of\_gen$  ( Using Eq. 10)
4.    $Fitness\_Val =$  Evaluating fitness (using algorithm 4)
5.    $P_1 =$  Selection ( $P_0$  ,  $Fitness\_Val$  ) (using algorithm 6)
6.    $Updat P_0$  using quantum rotation gate ( using algorithm 5 and defined Table 2)
7.   If (criteria is not false) then
8.     for  $j = 1$  to  $(P-1)$ 
```

9. P_2 = quantum crossover for $P_0(j)$ (using algorithm 7)
10. P_3 = quantum mutation for $P_2(j)$ (using algorithm 8)
11. endfor
12. endif
13. Evaluating and arranging individual population's fitness of P_j (using algorithm 4)
14. Select best individual with Elitism (using algorithm 9)
15. Select best environment with best individual (using algorithm 11)
16. endfor
17. Return (best individual with best environment)

The Quantum-Inspired Genetic Algorithm Using Dynamic Approach (QIGA2) is an innovative optimization approach that dynamically adjusts settings during execution. The process starts with initializing parameters, such as the minimum level (min_{Level}), maximum level (max_{Level}) determined using Equation 6, and initial level (Int_{Level}). The default chromosomal size is set at min_{Level} . The method refines the population through iterations at each incremental level (Int_{Level}).

In each iteration, quantum rotation gates update the quantum population $Q(t)$ depending on its prior state $Q(t-1)$, as specified in Table 2 (Algorithm 5). Algorithm 3 measures the quantum population to create a binary population ($P(t)$). This population is then subjected to quantum crossover (Algorithm 7) and mutation (Algorithm 8) to increase variety. Fitness is evaluated (Algorithm 4), and the best candidate is chosen through a selection procedure (Algorithm 6). Once a level's iterations are finished, the best individual from the current level is paired with the best individual from the previous level. The chromosomal size is increased by a predetermined interval (T), and the quantum population is reinitialized. The elitism mechanism (Algorithm 9) assures the survival of the top person while the best environment is selected (Algorithm 11). The process repeats for all levels up to max_{Level} . Finally, the method generates the best person and ideal environment, dynamically improving solutions via adaptive chromosomal sizing and quantum-inspired operations.

```

//Algorithm 2: QIGA Using Dynamic Approach (QIGA2) //
Input:  $min_{Level}$ ,  $max_{Level}$ ,  $Int_{Level}$ ,  $No\_of\_Iteration$ 
Output: Best individual with best environment
1. Initialized QIGA2 paraments ()
2. {
3.  $min_{Level} = 0$  (by default set)
4. calculate  $max_{Level}$  using Eq. 6
5.  $T =$  initialized interval
6.  $Int_{Level} = 1$  (by default set initial level)
7.  $t = 0$  (take temporary value)
8. }
9.  $Chromosome_{size} = min_{Level}$ 
10. for  $Int_{Level} = 1$  to  $max_{Level}$ 
11. {
12.     for  $i = 1$  to  $No\_of\_Iteration$ 
13.     {
14.         Updating  $Q(t)$  by using rotation gates applied to  $Q(t-1)$  as defined in Table 2.
          (using algorithm 6).
15.         Generate the binary population  $P(t)$  by measuring  $Q(t)$ . (using algorithm 3)

```

```

16.          Apply quantum crossover for P(t). (using algorithm 7)
17.          Apply quantum mutation process for P(t). (using algorithm 8)
18.          Evaluate the fitness of P(t) and select the best individual. (using algorithm 4
and 7)
19.          Increase i by 1.
20.          }
21. endfor
22.  Reset t to 0.
23.  Increase  $Int_{Level}$  by 1.
24.   $Best\_Individual(Int_{Level}) = Best\_Individual(Int_{Level} - 1)$  // Assign the top
performer (best individual) from the current level to the top performer (best individual) from
the prior level//
25.   $Chromosome_{size} = Chromosome_{size} + T$  // (increase size of chromosome by predefine
as interval) //
26.  Reinitialize the quantum population Q(t).
27.  Select best individual with Elitism (using algorithm 9)
28.  Select best environment with best individual (using algorithm 11)
29. }
30. endfor
31. Return (Best individual with best environment)

```

4.3 Initialization of Population- Algorithm 3 creates the initial population (P_0) for optimization. The approach starts with an empty population and estimates the max pooling layer (N_{PL}) size as $\log_2 d$, where d is the size of the training dataset. For each person in the population (N), it initializes N_{PL}^i to zero and creates a random number of blocks within the range (N_{min}, N_{max}). Empty arrays are built to contain block and connection IDs (Block_IDs) and active nodes.

Random blocks are chosen from each block, and if they belong to the pooling layer, N_{PL}^i is increased. If N_{PL}^i exceeds N_{PL} , alternate blocks and connections are produced to maintain validity. Connections and block IDs between random blocks are computed, and the best combination of block IDs and active nodes is selected. The ideal combination ($Comb_i$) is added to the population (P_0). After repeating the process for all N individuals, the population (P_0) is wholly initialized and ready for further processing.

```

// Algorithm 3: Initialization of population //
Input: size of population N, Minimum Node =  $N_{min}$ , Maximum Node =  $N_{max}$ , size of training
data set =  $d \times d$ , Pooling layer =  $N_{PL}$ 
Output: Initialized population  $N_0$ 
1.  $P_0 = \emptyset$ 
2. size of max pooling layer  $N_{PL} = \log_2 d$ 
3. for  $i = 1$  to N
4.    $N_{PL}^i = 0$ 
5.   temp = uniformly generate number between  $N_{min}$  and  $N_{max}$ 
6.    $Block\_IDs =$  create empty array (temp, temp) to store block and connection IDs
7.    $Block\_Active =$  create empty array size temp to store active nodes
8.   for  $j = 1$  to temp
9.     rand = choose random block
10.    If ( $b \in$  pooling block)
11.     $N_{PL}^i = N_{PL}^i + 1$  ( increase by one)

```

12. If $N_{PL}^i > N_{PL}$
13. $rand_1 =$ select block remaining block list
14. $rand_2(m, n) =$ randomly generate connection IDs between block m and n
15. $rand_3 =$ calculate $Block_IDs$ between two random block m and n
16. endfor
17. $Comb_i =$ get optimal (best) from array $Block_IDs$ and $Block_Active$
18. $P_0 = P_0 \cup Comb_i$
19. endfor
20. return P_0

4.4 Quantum Fitness Process- Fitness evaluation provides a quantitative assessment to identify individuals eligible for parental roles. Algorithm 4 illustrates the framework for fitness evaluation in QIGA. QIGA addresses image classification tasks, making classification errors the most effective criterion for determining fitness.

Each represented quantum circuit is trained on the training set D_{Train} , while the fitness is evaluated on a separate dataset $D_{Fitness}$. Quantum circuits often possess deep architectures, necessitating substantial computational resources and extended time for thorough training to achieve minimal classification error. A complete training process typically involves many epochs, with 100 epochs being standard for quantum circuit training. This will render the situation considerably more impractical due to the population-based QGAs involving multiple generations, wherein each individual undergoes complete training in each generation. In this method, each undergoes training for a predetermined average of epochs, specifically 100 epochs, tailored to their architectures and connection weight initialization values. Subsequently, the mean value and standard deviation of classification error are computed for each batch of $D_{Fitness}$ in the final epoch. The mean value and standard deviation of classification errors are utilized as an individual's fitness measure. A smaller mean value indicates a superior individual. When individuals being compared have identical mean values, a lower standard deviation signifies an exceptional outcome.

// Algorithm 4: Evaluate fitness for quantum population //

Input: Set of Population $P_N = \{P_0, P_1, P_2, \dots, P_{N-1}\}$, $q =$ number of qubits, $Total_Epoch =$ number of training epochs or size of batch, $D_{Train} =$ set of training dataset, $D_{Fitness} =$ set of evaluate dataset, $Measure_Acc =$ measurement of accuracy with training epochs

Output: Fitness F with individual population

1. Construct quantum circuit
2. Evaluating training dataset with quantum circuit
3. Initialization quantum logic gate with quantum $\delta_N = \{\delta_0, \delta_1, \dots, \delta_{N-1}\}$
where $\delta_0 = \{\theta_0, \theta_1, \dots, \theta_{N-1}\}$
4. for each individual κ in P_N
5. $i=1$
6. $every_step_i = \frac{|D_{Fitness}|}{Total_Epoch}$
7. while ($i \leq Measure_Acc$)
8. Train connecting by weights of quantum with individual κ
9. Training quantum by gradient descent optimizer and set $\delta_N \rightarrow \delta_N'$
10. If ($i == Measure_Acc$)
11. $AccList = \emptyset$
12. for $j=1$ to $every_step$

```

13.           $Acc_j$  = evaluating classification error for  $D_{Fitness}$ 
14.          If (  $Acc_j$  is valid for current quantum circuit )
15.               $Acc_{List} = Acc_{List} \cup Acc_j$ 
16.               $j=j+1$ 
17.          endfor
18.      update  $\kappa$  from  $P_N$ 
19.  endwhile
20.   $i=i+1$ 
21. endfor
22. return (fitness F for current population P)

```

4.5 Quantum Rotation Gate- In contrast to the GA, the QGA utilizes the probability amplitude of qubits for chromosome encoding and employs quantum rotating gates (QRGs) to execute chromosomal update operations. The parental group does not decide the generation of offspring when QRGs are used to perform genetic operations due to the chromosomes being in a state of superposition (entanglement). The optimal individual of the parental group and the probability amplitude of each state collectively establish it. The genetic manipulation of QGAs mainly involves altering the superposition or entanglement states through QRGs to modify the probability amplitude. Consequently, the development of QRGs (using algorithm 5) is a critical aspect of QGAs, significantly influencing the algorithm's performance.

QRGs can be engineered to address practical issues and are typically characterized as –

$$U(\theta_i) = \begin{bmatrix} \cos \theta_i & -\sin \theta_i \\ \sin \theta_i & \cos \theta_i \end{bmatrix} \quad [7]$$

Then updated process is

$$\begin{bmatrix} a'_i \\ b'_i \end{bmatrix} = U(\theta_i) \begin{bmatrix} a_i \\ b_i \end{bmatrix} = \begin{bmatrix} \cos \theta_i & -\sin \theta_i \\ \sin \theta_i & \cos \theta_i \end{bmatrix} \begin{bmatrix} a_i \\ b_i \end{bmatrix} \quad [8]$$

Where $[a_i \ b_i]^T$ is probability amplitudes of i th qubit of chromosome before rotating of quantum gate. After rotation and updating quantum gate through algorithm 5 and represent as $[a'_i \ b'_i]^T$ for i th qubit of chromosome. The rotation angle denoted by θ_i for i th qubit and adjustment follow gate adjustment strategy (show in table 2), which is determined as $S(a_i, b_i)$ respectively. Where $S(a, b)\Delta\theta_i$ is defined direction of rotation (sign) and $\Delta\theta_i$ is rotation angle values (show in table 2). $\Delta\theta_i$ and $S(a_i, b_i)$ give lookup tables 2. Where $f(x)$ is representing fitness of binary (0 or 1) chromosomes x and $f(b)$ is represent best fit of individual chromosomes. The values of θ_i is adjust by gate strategy and we perform task on different values and show best fit, average fit, and random fit in table 2. the fitness values $f(x)$ evaluated for current chromosome x and compared with optimal fit $f(b)$ values. If $f(x)$ is greater than $f(b)$ then qubit adjust to direction of x with probability (a_i, b_i) for i th qubit. If $f(x)$ is less than $f(b)$ then qubit adjust to direction of best with probability (a_i, b_i) for i th qubit.

The rotation angle is adjusted by following formula-

$$\Delta\theta_i = \theta_j - \left(\frac{\theta_j - \theta_i}{\text{Number of Repetition (per level)}} \right) * \text{Epochs} \quad [9]$$

Where rotation's sign of θ_j and θ_i will be calculating with theorem 1 and 2.

x_i	b_i	$f(x) \geq f(b)$	$S(\alpha_i, \beta_i)$												$\Delta\theta_i$			Apply Theorem		
			$\alpha_i, \beta_i > 0$			$\alpha_i, \beta_i < 0$			$\alpha_i = 0$			$\beta_i = 0$			T1	T2	T3	T1	T2	T3
			T1	T2	T3	T1	T2	T3	T1	T2	T3	T1	T2	T3						
0	0	False	0	-	-	0	+	+	0	±	±	0	±	0	0	$\Delta\theta_1$	$\Delta\theta_1$	-	1 and 2	1 and 2
0	0	True	0	-	-	0	+	+	0	±	±	0	±	0	0	$\Delta\theta_1$	$\Delta\theta_1$	-	1 and 2	1 and 2
0	1	False	0	-	+	0	+	+	0	±	0	0	±	±	0	$\Delta\theta_3$	$\Delta\theta_1$	-	1 and 2	1 and 2
0	1	True	-	-	-	+	+	+	±	±	±	0	±	0	$\Delta\theta_2$	$\Delta\theta_2$	$\Delta\theta_1$	1 and 2	1 and 2	1 and 2
1	0	False	-	+	-	+	-	-	±	±	±	0	±	0	$\Delta\theta_1$	$\Delta\theta_1$	$\Delta\theta_1$	1 and 2	1 and 2	1 and 2
1	0	True	+	+	+	-	-	+	0	±	0	±	±	±	$\Delta\theta_3$	$\Delta\theta_3$	$\Delta\theta_1$	1 and 2	1 and 2	1 and 2
1	1	False	+	+	+	-	-	+	0	±	0	±	±	±	$\Delta\theta_1$	$\Delta\theta_1$	$\Delta\theta_1$	1 and 2	1 and 2	1 and 2
1	1	True	+	+	+	-	-	-	0	±	0	±	±	±	$\Delta\theta_3$	$\Delta\theta_1$	$\Delta\theta_1$	1 and 2	1 and 2	1 and 2

Table 2: Lookup Table of rotation angle with rotation direction (Test case -T1, T2, and T3) (1- Theorem 1 and 2- Theorem 2)

4.5.1 Generation Distribution Across Various Precision Levels

Due to QIGA's utilization of varying chromosomal sizes throughout execution, allocating a specific number of generations to each level is necessary. Shorter chromosomes necessitate fewer generations compared to those with a more significant number of genes. They are utilizing a low level of accuracy, resulting in a significantly reduced number of potential solutions compared to greater accuracy levels. Consequently, the algorithm's generations are allocated across various levels, such that when accuracy improves, the quantity of generations associated with those levels escalates. The number of repeats at each level is specified by Equation 10.

$$\text{Number of Repetition (per level)} = \frac{\text{Level}_{no}}{\text{Max}(k+1)/2} \times m \quad [10]$$

Where Level_{no} = number of levels

m = number of iterations

k = maximum length of level

$$m = \sum_{i=1}^{\text{Level}_{no}} \text{Repetition_Process}_i$$

// Algorithm 5: Updating of quantum states //
 Input: Population size P
 Output: update quantum state

```

1. i=0
2. while (i<N)
3.     evaluate ith gene of best individual of population and store in Best_Amp (using
       algorithm 10 and 12)
4.     k=0
5.     j=0
6.     While (j<2)
7.         If (j! = Best_Amp )
8.             Q[j]= c*Q      /*where c is any constant and c ∈[0,1] */
9.             k= k+ Q[k]2
10.        endif
11.       j=j+1
12.     endwhile
13.     Q[inBest_Amp] = √(1-k)
14.     i=i+1
15. endwhile

```

Updating Quantum States (Algorithm 5) refines a population's quantum state using the genes of the best individuals. The algorithm analyses the best gene for each person in the population and records its amplitude in Best_Amp (using Algorithms 10 and 12). The algorithm iterates across quantum states $Q[j]$, scaling any states that do not meet Best_Amp with a constant $c \in [0,1]$. The cumulative probability (k) for these states is updated. Finally, the optimal gene's amplitude is computed as $1 - k$. This procedure is repeated for all people, updating the quantum states to reflect the effect of the top-performing individual.

4.6 Selection Process- The Binary Tournament Selection algorithm (Algorithm 6) picks individuals based on their mean and parameter values. It begins by organizing the mean values of individuals in descending order (σ'_N). Two random mean values, σ_i , and σ_j , are picked. If both are maximal, the mean (μ_1, μ_2), standard deviation ($Stad_1, Stand_2$), and parameters ($Y_1 - Y_2$) are assessed. The program evaluates the difference in mean values ($\mu_1 - \mu_2$) to a threshold (σ) and picks the individual with the greater mean. If the difference in parameters ($Y_1 - Y_2$) exceeds the threshold β and $Stad_1 > Stand_2$, then σ_j is picked; otherwise, σ_i is chosen. If σ_i and σ_j are not the maximum, one is randomly selected. This step is repeated to complete the selection.

```

// Algorithm 6: Binary tournament selection //
Input: Set of individuals,  $\alpha$  = Threshold value of mean,  $\beta$  = Threshold value of parameter
       numbers, set of individuals with mean value  $\sigma_N = \{\sigma_0, \sigma_1, \dots, \sigma_{N-1}\}$ 
Output: selected only Individual
1. Arrange set of mean value in decreasing order and store in  $\sigma'_N$ 
2. Select two random mean values  $\sigma_i$  and  $\sigma_j$ 
3. if ( $\sigma_i$  and  $\sigma_j$  are both are maximum)
4.      $\mu_1$  and  $\mu_2 \leftarrow$  Evaluated mean value of  $\sigma_i$  and  $\sigma_j$ 
5.      $Stad_1$  and  $Stand_2 \leftarrow$  Evaluated standard derivation value of  $\sigma_i$  and  $\sigma_j$ 
6.      $Y_1$  and  $Y_2 \leftarrow$  Select two parameters of  $\sigma_i$  and  $\sigma_j$ 
7.     If ( $(\mu_1 - \mu_2) > \sigma$ )
8.         return  $\sigma_i$ 

```

```

9.     elseif ((( $Y_1 - Y_2$ ) >  $\beta$ ) and ( $Stand_1 > Stand_2$ ))
10.    return  $\sigma_j$ 
11.    else
12.    return  $\sigma_i$ 
13.    endif
14. else
15.    return random one from  $\sigma_i$  and  $\sigma_j$ 
16. endif
17. repeat step 2 to 16

```

4.7 Quantum Crossover Process- The Quantum Crossover Process (Algorithm 7) creates children by merging genes from two parent people. Two random genes ($P_{Gen,i}$ and $P_{Gen,j}$) are taken from the parent gene set (P_{Gen}). Gene segments ($Temp_1$ and $Temp_2$) are retrieved from randomly chosen places (Pos_1 and Pos_2) within these genes. The authenticity of the selected gene segments is verified; if so, they are assessed, edited, and united to produce a new offspring. If the chosen genes are invalid, the procedure is repeated until valid genes are discovered. The resultant offspring is returned as $Offspring_{Gen}$.

// Algorithm 7: Quantum Crossover Process //

Input: Set of gene parent P_{Gen}

Output: Set of offsprings $Offspring_{Gen}$ (generated by algorithm 10 and 12)

```

1.  $P_{Gen,i}$  and  $P_{Gen,j} \leftarrow$  Select rand two gen from set of gen parent  $P_{Gen}$ 
2.  $Pos_1 \leftarrow$  Select random position in  $P_{Gen,i}$ 
3.  $Pos_2 \leftarrow$  Select random position in  $P_{Gen,j}$ 
4.  $Temp_1 \leftarrow$  select random gen from parent  $P_{Gen,i}$  with position  $Pos_1$ 
5.  $Temp_2 \leftarrow$  select random gen from parent  $P_{Gen,j}$  with position  $Pos_2$ 
6. check validation of selected random gen  $Temp_1$  and  $Temp_2$ 
7. if ( $Temp_1$  and  $Temp_2 = Valid$ )
8.    Evaluate, modified, combined and create new offspring
9.     $Offspring_{Gen} =$  new offspring
10. else
11.    Goto step 4
12. endif
13. return  $Offspring_{Gen}$ 

```

4.8 Quantum Mutation Process- The Quantum Mutation Process alters the genetic structure of people in a population using predetermined mutation operations and a mutation rate. The method starts by iterating through each gene in the individual. For each gene, a random probability is calculated, and if it is smaller than the mutation rate, a mutation occurs at a randomly chosen place within the gene.

Depending on the type supplied, a variety of mutation procedures are available. If the operation is Addition, a random gene (bit) is picked and placed at the specified spot. Remove selects and removes a block from the gene. If Modified is selected, a random block is changed with a new one at the given point. Swap involves selecting two genes ($P_{rand,i}$ and $P_{rand,j}$ line-13 in algorithm 8) and swapping their order if they appear in the same gene. The Inversion process

involves repeatedly swapping genes between two defined places ($P_{rand,temp1}$ and $P_{rand,temp2}$, in line 18-21 in Algorithm 8) until the range is reversed. When Scramble is selected, the genes between two randomly chosen places are scrambled, resulting in a random rearrangement of the gene sequence.

When the mutation process is finished for all genes in the person, the mutated individual is returned as the output, including the newly transformed genetic material. This approach promotes greater variety and exploration of the solution space, which is essential in GA.

```

// Algorithm 8: Quantum Mutation Process//
Input: Set of parent P, Set of block n in P, Types of Operation= Addition, Remove, Modified, Swap,
Inversion, Scramble, Mutation_Rate
Output: Set of Mutated offspring
1. For each gene in individual
2.   If (random probability < Mutation_Rate)
3.     {
4.        $P_{rand} \leftarrow$  Select any random position for mutation
5.       if (Types_Operation= Addition)
6.         Perform Addition Operation : select random gene (bit) and insert in  $P_{rand}$ 
7.       else if (Types_Operation = Remove)
8.         Perform Remove Operation : select block and remove from n
9.       else if (Types_Operation = Modified)
10.        Perform Modified Operation = select random block and put into  $P_{rand}$ 
11.      else if (Types_Operation = Swap)
12.        If ( $P_{rand,i}$  and  $P_{rand,j} \in n$ )
13.          Perform Swap Operation = swap (  $P_{rand,i}$  and  $P_{rand,j}$ )
14.      else if (Types_Operation = Inversion)
15.         $P_{rand,temp1} \leftarrow$  define initial position of block
16.         $P_{rand,temp2} \leftarrow$  define last position of block
17.        while ( $P_{rand,temp1} < P_{rand,temp2}$ )
18.          {
19.            Swap ( $P_{rand,temp1}$  and  $P_{rand,temp2}$  )
20.             $P_{rand,temp1} = P_{rand,temp1} + 1$ 
21.             $P_{rand,temp2} = P_{rand,temp2} - 1$ 
22.          }
23.        endwhile
24.      else if (Types_Operation = Scramble)
25.        shuffle (n,  $P_{rand,temp1}$ ,  $P_{rand,temp2}$ )
26.        if(  $P_{rand,temp1} > 1$  and  $P_{rand,temp2} < n$ )
27.          {
28.            for i =  $P_{rand,temp1}$  to  $P_{rand,temp2}$ 
29.              temp = i + rand ()/ (rand_max/ ( $P_{rand,temp2} - i + 1$ ))
30.              Swap ( $P_{rand,temp1}$ , temp)
31.            }
32.          }
33.    endfor
34.  return individual

```

4.9 Elitism Theory - The Elitism algorithm (Algorithm 9) in QGAs is concerned with preserving the population's top performers and guaranteeing their survival throughout generations. The approach begins by picking weights for two quantum populations (QW_i and QW_j) from a collection of quantum weights (QW). Next, the sizes of the updated quantum population ($QD_{updated}$) and QD_j are specified as N and M, respectively. A temporary variable, Temp, is formed by combining a random value and the difference between QW_i and QW_j . If an individual D_i 's fitness is lower than an individual D_j 's, weight QW_i is updated by adding Temp. Otherwise, QW_j updates identically. This step returns the updated quantum weights ($QW_{updated}$).

```

// Algorithm 9: Elitism in Quantum Genetic Algorithms//
1. Select two quantum population's weight  $QW_i$  and  $QW_j$ 
2.  $QW_i$  and  $QW_j \in QW$ 
3. N= size of  $QD_{updated}$ 
4. M= size of  $QD_j$ 
5. Temp= mod (rand (  $QW_j - QW_i$ ))
6. if (  $\sigma_{D_i} < \sigma_{D_j}$ )
7.    $QW_i = QW_i + \text{Temp}$ 
8. else
9.    $QW_j = QW_j + \text{Temp}$ 
10. endif
11. return set of updated  $QW_{updated}$ 
12. for all  $QW_j \in QW_{updated}$ 
13.   while ( i < N+1) do
14.     while (j < M+1) do
15.        $QW_{(i,j)} = \max\_val(QW_{(i,j)}) + \min\_val(QW_{(i,j)}) - QW_{(i,j)}$ 
16.       j=j+1
17.     endwhile
18.     i=i+1
19.   endwhile
20. delete all duplicated  $QW_{updated}$  from set of  $QW_{updated}$  and keep identical
21. select optimal  $QW_{updated}$  from set of  $QW_{updated}$ 
22. return optimal ( $QW_{updated}$ )

```

4.10 Generation of Offspring -The algorithm 10 for generating children comprises picking pairs of parents from the population and producing offspring via crossover processes and mutation processes. First, two random parents (P_i and P_j) are chosen from the population (P_N). The algorithm will proceed if both parents are in the mating pool ρ . The selected parents produce offspring using the crossover operator (as explained in Algorithm 7). Once offspring are formed, they are validated using Algorithm 12. If the children are legitimate, the mutation operator (from Algorithm 8) adds genetic variety. The children from both parents are added to the collection of offspring. The parents, P_i and P_j , are removed from the mating pool. The selection, mutation, and crossover stages are repeated until the mating pool is empty.

After iterating over the population and conducting crossover and mutation operations to pairs of parents from the mating pool, the end outcome is the set of offspring (ζ). This guarantees that the population develops and adds new variants to the following generation. The pseudocode for generation of offspring is demonstrated in algorithm 10.

// Algorithm 10: Generating offspring //

Input: Set of Population $P_N = \{P_0, P_1, P_2, \dots, P_{N-1}\}$, Mating Pool ρ
Output: Set of offspring ζ

1. Select two random parents P_i and P_j
2. If (P_i and $P_j \in P_N$)
3. If (P_i and $P_j \in \rho$)
4. generate offspring by using crossover operator (using algorithm 7)
5. If (offspring is valid) then (using algorithm 12)
6. generate offspring by using mutation operator (using algorithm 8)
7. $\zeta = \zeta_i \cup \zeta_j$ (store offspring)
8. delete both parents P_i and P_j from mating pool
9. Repeat step 1 to 8 until mating pool are not empty.

4.11 Selection of Best Environment- The environmental selection process explicitly addresses elitism and diversity (using algorithm 9). A subset of individuals with favourable mean values is selected initially, followed by selecting the remaining individuals using the modified binary tournament selection method outlined in Algorithm 6. The proposed QIGA method aims to enhance performance by simultaneously considering elitism and diversity through these two strategies.

The algorithm 11 for population selection using elitism and genetic operators focuses on generating a new population P_{F+1} by combining the best individuals from the current population P_F and the offspring Q_F . Initially, the number of elite individuals is determined using the elitism relative to the population size N . The top-performing individuals (with the best mean values) are selected as elites and added to P_{F+1} . Offspring Q_F is generated using genetic operators, such as mutation and crossover. The union of P_{F+1} and Q_F is evaluated to identify optimal individuals for inclusion in P_{F+1} .

For further selection, two random individuals, $rand_1$ and $rand_2$, are chosen based on their means and standard deviations. If the mean difference (μ_1 and μ_2) exceeds a threshold ϵ , or if one individual's standard deviation is smaller (indicating stability), it is selected. Otherwise, the algorithm randomly chooses between $rand_1$ and $rand_2$. This selected individual is stored temporarily. The process repeats iteratively until the size of P_{F+1} matches N , ensuring a balanced representation of elites and offspring while maintaining diversity and fitness. The final P_{F+1} is returned as the next generation of the population.

// Algorithm 11: Selection of appropriate environment //

Input: Elitism fraction, size of population P
Output: Select population P_{F+1}

1. temp= calculate number of elites by using Elitism with the respect to size of population N (using algorithm 9)
2. P_{F+1} = select the best (optimal) temp value, which is give best mean value in $P_F \cup Q_F$

3. Q_F = generating offsprings with genetic operator/
4. ϵ = mean threshold value
5. $P_F \cup Q_F = (P_F \cup Q_F) + P_{F+1}$
6. Select two random values $rand_1$ and $rand_2$
7. / $rand_1$ is selected individual value with maximum mean and $rand_2$ is another value with another maximum mean, where $rand_1$ and $rand_2 \in \hat{u}$ (\hat{u} is set of mean values with individual values)
8. Select standard deviation std_1 and std_2 of $rand_1$ and $rand_2$ respectively
9. Select mean value μ_1 and μ_2 of $rand_1$ and $rand_2$ respectively
10. If $(\mu_1 - \mu_2 > \epsilon)$
11. Return $rand_1$
12. else if $(std_1 < std_2)$
13. return $rand_1$
14. else if $(std_1 < std_2)$
15. return $rand_2$
16. else
17. return select random between ($rand_1$ and $rand_2$) and store in $temp_2$
18. While $(|P_{F+1}| < N)$ do
19. select temp value using step 5 to 16
20. $P_{F+1} = P_{F+1} \cup temp_2$
21. endwhile
22. return P_{F+1}

4.12 Filter Feature Selection and Extraction Process- The feature selection techniques may be broadly divided into filter and selection approaches based on the feature estimation procedure. In the filter techniques, the features are assessed independently of a classifier according to specific criteria. In contrast, the wrapper approach uses a classifier to determine the most advantageous features.

This article used three popular filter methods to calculate a score for each feature: information gain and gain ratio. In order to scall down the high dimensional benchmark datasets, only the top 10% of ranking features were later selected, with the remaining redundant or unnecessary characteristics being removed.

(a) Information Gain (IG)-IG is one of the widely used filtering strategies that has been effectively used to choose more precise relevant features in numerous applications to decrease high-dimensional benchmark datasets. By computing the information gain of features about class labels, the Information gain employs the entropy (*Entrpy* (S)) measure to assess the importance of features. Equation (11) is utilized in the information gain to determine the features:

$$InfGain(S, F) = Entrpy(S) - \sum_{i \in F} \frac{|S_i|}{|S|} Entrpy(S_i) \quad [11]$$

Where F = Value of selected set of features

S = Choose dataset and $S_i \subseteq S$.

S_i = Selected i^{th} sub-dataset after splitting of choosing dataset S .

Entropy (S) can be compute by equation (12)

$$Entropy(S) = -\sum_{i=1}^N p_i \log_2 p_i \quad [12]$$

The log to base 2 of a selected category's probability (p_i) describes the uncertainty or impurity. The number of potential categories is indicated by the index (i), which is dependent on a number of features.

The Information gain is frequently used to determine a feature's level of significance. However, Information gain might have an overfitting issue because it is inclined toward features with a wide range of values.

(b) Information Gain Ratio (IGR)- By considering the quantity and size of branches while selecting an attribute, the IGR was created to enhance information gain performance and lessen its bias toward high-branch qualities. Equations (13) and (14) are used, respectively, to assess the properties of the information gain ratio and split information:

$$InfGain_ratio(S, F) = \frac{InfGain(S, F)}{Spilt_info(S, F)} \quad [13]$$

$$Spilt_info(S, F) = -\sum_{i=1}^N \left(\frac{|S_i|}{|S|} \right) \log_2 \left(\frac{|S_i|}{|S|} \right) \quad [14]$$

4.13 Quantum Genetic Algorithm (QGA)-based Filter Feature Selection and Extraction Process

The characteristics obtained from the preceding phase are organized sequentially from the initial image in the matrix to the final image, with the feature vector comprising the primary features of each descriptor. This study utilizes a feature vector of length 784 (28x28), which is input into QIGA for feature selection. In QIGA, the qubit representation was utilized for reduction problems and grounded in quantum computing concepts. The representation's property is that any linear superposition can be depicted. The state of a qubit can be expressed as follows: U represents an arbitrary single-qubit unitary operation, and θ_i denotes the rotation angle for each qubit about the y-axis, defined as:

$$\theta_i = S(\alpha_n, \beta_n) * \Delta \theta_i \quad [15]$$

Where $S(\theta_n, \theta_n)$ is show sign of θ_i . θ_i is the indicator that determines the direction of angle, and $\Delta \theta_i$ is the magnitude of the rotation gate. θ_i must supply the rotation angle in radians, which may be positive or negative. α'_n and β'_n are computed as:

$$\begin{bmatrix} \alpha'_n \\ \beta'_n \end{bmatrix} = U(\theta) \begin{bmatrix} \alpha_n \\ \beta_n \end{bmatrix} \quad [16]$$

The initial feature selection phase randomly initializes the population and evaluates its value through the fitness function. The precision of classification serves as a fitness function. The initial population is subsequently input into the quantum gate. A chromosome is logically identical to an n-qubit string of quantum states. All qubits can be adjusted to the identical value of $1/\sqrt{2}$, indicating that all fundamental quantum states are quantum superpositions with equivalent probabilities. The fitness function is utilized to evaluate the new quantum

population. To obtain a decimal value from a quantum population, the state of each individual is transformed from decimal to binary string before the assessment. The random are generated and every gen assign with 0 or 1.

Subsequently, the weight configuration of the solution and its fitness value will be preserved. The optimal tree and its suitability and binary solution $P(t)$ are already designated and archived for further generations. The renewal policy aims to align the fitness $f(x_i)$ of the recently assessed item rate with the current meta-heuristic goal's fitness $f(b_i)$. If $f(x_i) > f(b_i)$, then adjust the qubit corresponding to $f(x_i)$ to enhance the probability of x_i 's occurrence. Conversely, if $f(x_i) < f(b_i)$, adjust the qubit of the corresponding bit to achieve the amplitude (probability) scale and proceed in the direction of advocate the existence of b_i . Additionally, α is the angle increment of the update. The α value affects the convergence rate: A significant number may cause the resolution to prematurely diverge or converge to a particular optimum. The dynamic adjustment of α is sanctioned, allowing it to attain values between 0.001π , 0.05π , and 0.08π , as determined by the variance of genetic generations.

The four main steps of feature selection based on QIGA are typically population initialization (using algorithm 3), fitness evaluation (using algorithm 4), chromosome encoding (using algorithm 5), and reproduction (selection using algorithm 6), crossover (using algorithm 7), and mutation (using algorithm 8).

QIGA iteratively develops the chromosomes to generate a new generation of improved solutions by repeating the reproduction and fitness evaluation procedure until QIGA meets one of the termination requirements, such as reaching maximum generations or attaining adequately optimal fitness. Algorithm 12 shows the pseudocode for the feature selection approach based on GAs.

// Algorithm 12: Genetic-based feature selection and extraction //

Input: Set of all features, size of chromosome=N

Output: Best feature

1. Evaluating Feature's score using Eq. 11-14
2. Arrange all feature's score in descending order
3. Select only top score // in our experiment, we set top score 10%. //
4. Dim = Evaluating dimension of selected top feature
5. Initialization of population (using algorithm 3)
6. Generating chromosomes N with Dim (selected of features 10%)
7. Each Dim (selected of features) with random values 0 or 1. //convert all chromosome with binary features (0 and 1)//
8. if (Dim=1)
9. while (condition not false)
10. Evaluating quantum fitness value (using algorithm 4)
11. Selection performs on selected two parents (using algorithm 6)
12. Perform quantum crossovers process (using algorithm 7)
13. Perform quantum mutation process (using algorithm 8)
14. endwhile
15. endif
16. Select best chromosomes
17. Select best feature from selected best chromosomes and store in *Best_Chromosome*
18. Return (*Best_Chromosome*)

This algorithm 12 aims to choose the most relevant characteristics from a set of all accessible filter, feature extraction, and selection using a GA. Initially, features are examined using a scoring method, with the top 10% of characteristics picked. These top features define the dimension (Dim) of chromosomes, with each chromosome being a binary representation of selected traits. The population is initiated by creating chromosomes with random binary values. If Dim equals 1, the evolutionary process begins, with each chromosome's fitness evaluated and parent selection, crossover, and mutation procedures repeated. Evolution continues until the termination condition is reached. Finally, the best-performing chromosomes are chosen, and the most significant characteristics from these chromosomes are saved in *Best_Chromosome*, which serves as the final output. This method optimizes feature subsets for better performance in machine learning tasks.

5. Experimental Setup and Result Discussion

First, we used prominent feature selection techniques—listed in the preceding section—whose recall fitness scores, accuracies, loss, and error are shown to assess our proposed method's performance. The proposed model was then matched with the outcomes.

The performance results of the suggested models employing the quantum-based-selected features are then shown. The evolutionary development of the proposed quantum-inspired genetic methodology using dynamic models is illustrated since it is iteration-based. Different datasets and test cases allow the best fitness and average solutions from the feature selection models to be shown in a comparison analysis.

5.1 Quantum Simulators

Quantum simulators are engineered to replicate quantum working environments on traditional system. A quantum simulator replicates qubits, quantum-circuits, and environments as authentic quantum computers. To facilitate the study and construction of quantum algorithms, numerous prominent corporations and scientific research organizations have created an array of quantum simulators, such as Google Collab, VS Code, and IBM-Qiskit. Qiskit offers customers an extensive array of quantum logic gate interfaces and techniques for manipulating qubits, enabling precise control over quantum circuits.

In the proposed QIGA method, we use Qiskit, VS-code and collab for quantum circuit construction and quantum environment simulation. We summarize basic hardware and software requirements for our experimental setup in Table 3.

Attributes	Descriptions
System	MacBook Air M2
MacOS	Sequoia 15.0
RAM	16 GB (LPDDR5)
SSD	512 GB
CPU	8-Core (4- high performance @ 3.49 GHz, 4- energy efficiency @ 2.42 GHz)
GPU	10-Core
GPU	500 MHz (clock base), 1398 MHz (Boost Clock)
Clocks	6400 MHz

Simulator	Qiskit, Google Colab, VS Code
Language	Python

Table 3: Basic System Requirement

5.2 Simulation and Parameters Setup

The primary aim of this paper is to developed a dynamic model discovery algorithm for researchers' area expertise in quantum technology. Enhancing the applicability of the proposed quantum-based model is intended to ensure that potential users do not need expertise in QIGA. Therefore, we establish required parameters of the proposed algorithm according to established conventions. The probabilities of crossover and mutation are detailed in Table 4. We examine three distinct test cases—1, 2, and 3—for GA, QIGA1, and QIGA2 while specifying their parameters in Table 4.

Parameters	Values for GA, QIGA1, and QIGA1		
	Test 1	Test 2	Test 3
Test No	Test 1	Test 2	Test 3
Size of Population	50	50	50
Number of Epochs	100	100	100
Probability of crossover	0.2	0.4	0.6
Probability of mutation	0.5	0.6	0.8
Rotation Angle	0.001π	0.05π	0.08π
Mutation Type	Uniformly	Uniformly	Uniformly
Selection Type	Binary	Binary	Binary

Table 4: Test cases with their parameters

5.3 Benchmark Datasets

Partially drawn from MNIST's training and testing datasets, the MNIST database includes 10,000 28x28 pixel testing and 60,000 training pictures. A similar structure is provided by the Fashion MNIST dataset, a subset of MNIST that has 10,000 testing and 60,000 training 28x28 grayscale pictures divided into 10 groups. An expansion of the NIST Special Dataset 19, the EMNIST Digits dataset consists of 240,000 training and 40,000 testing 28x28 pictures containing digits, capital and lowercase letters, and parameters structured similarly to MNIST. A 32x32 RGB image classification benchmark for ten classes, including birds and airplanes, the CIFAR-10 dataset consists of 10,000 testing and 50,000 training pictures, with equal samples in each category. Based on an expanded collection of original color pictures, the Sign-MNIST dataset contains 27,455 training and 7,172 testing 28x28 grayscale images of hand motions representing American Sign Language letters (J and Z are omitted owing to mobility limits). All dataset's specific parameters are shown in Table 5.

Table 5 delineates the attributes of the Fashion MNIST, MNIST, EMNIST Digits, CIFAR-10, and Sign MNIST datasets concerning training and test samples and the number of classes.

Datasets	Training Samples	Testing Samples	Classes
Fashion MNIST	60,000	10,000	10
MNIST	60,000	10,000	10
DIGITS MNIST	240,000	40,000	10
CIFAR-10	50000	10000	10
Sign MNIST	27455	7172	10

Table 5: Dataset with their parameters

5.4 Result

This section compares the performances of quantum machine learning (QML) techniques utilizing the proposed featured extraction and filter-based GA selection method against standalone quantum-based learning techniques and genetic techniques, focusing solely on filter, feature extraction, and selection methods.

Figures 4–43 and Tables 6–8 compare the best fitness, average fitness, accuracy, and loss results for quantum-inspired genetic techniques. This comparison utilizes features selected solely by filter and features method are selected by the proposed dynamic QIGA model across five high-dimensional datasets: MNIST, Fashion-MNIST, Digit-MNIST, Sign-MNIST, and CIFAR-10. The filter methods yielded optimal classification results when quantum-based learning techniques were trained using the top 10% of ranked features across five datasets. The proposed dynamic QIGA (1 and 2) feature and filter selection method further enhanced classification accuracies and best and average fitness while also improving loss. We examine three types of cases.

5.4.1 Comparative Analysis of Fitness and Accuracy, and Loss

We perform three different analyses based on GA, QIGA1, and QIGA2 for five types of MNIST datasets with three test cases.

Analysis of Conventional Genetic Algorithm (GA) for MNIST datasets- We calculate the GA best and average fitness, accuracy, and loss for three quantum machine learning test cases trained on MNIST datasets. We tabulate the result for all cases in Table 6–8 and demonstrate it in Fig. 4-43. We note average and best fitness scores range from 0.9534 to 0.9699 and 0.9498 to 0.9663, accuracy range from 0.9598 to 0.9769, and loss range from 0.3517 to 0.5878 for all three test cases.

Analysis of Feature selection and Extraction based- QGA for MNIST datasets- Now, we add feature extraction with a GA with a quantum approach for image classification called the Feature-based quantum-inspired genetic algorithm (QIGA1). The result of QIGA1 is shown in Table 6–8 and demonstrated in Figure 4-43. The QIGA1 increased fitness and accuracy and reduced loss from GA approx.by 2% - 3%, 2%- 4%, and nearly 2%-10%, respectively. The best and average fitness, accuracy, and loss achieved by QIGA1 range from 0.9874 to 0.9899, from 0.9853 to 0.9874, from 0.9891 to 0.9988, and from 0.0387 to 0.0622, respectively, for all three test cases and summarized in Table 6–8 and demonstrated in Fig. 4-43.

Analysis of Feature Selection and Extraction with Dynamic Approach for MNIST datasets – We have now updated the previously proposed model (QIGA1) with a dynamic approach called a dynamic quantum-inspired genetic algorithm (QIGA2). This method continuously updates rotation angles, mutation, and crossover with dynamic and improved results. The results are summarized in Table 6–8 and demonstrated in Fig 4-43. This dynamic approach increases fitness, accuracy, and reduced loss approx.by 3%-4%, 2%-4%, 2%-4%, and 4%-11% for GA and 1%-2%, 1%-2%, 1%-2%, and 1%-3% for QIGA1 for all three test cases, and the overall results are summarized in Table 6–8 and demonstrated in Fig. 4-43.

Tables 6 and 7 present the classification accuracy alongside performance metrics such as Recall and Precision, as well as the best and average fitness and loss measures for GA, QIGA1, and QIGA2, both before and after implementing the proposed dynamic filter and feature extraction and selection GA-based methods. Figures 4–43 and Tables 6-8 illustrate that in all three test cases, both GA and QIGA demonstrated superior performance after utilizing the proposed dynamic QGA method compared to classifiers employing alternative feature selection methods.

Database	Test No.	GA		QIGA-1		QIGA-2	
		Best-Fit	Avg-Fit	Best-Fit	Avg-Fit	Best-Fit	Avg-Fit
Fashion-MNIST	1	0.9534	0.9491	0.9736	0.9692	0.9989	0.9974
	2	0.9429	0.9347	0.9854	0.9771	0.9991	0.9967
	3	0.9523	0.9498	0.9888	0.9857	0.9992	0.9990
MNIST	1	0.9488	0.9393	0.9787	0.9748	0.9986	0.9972
	2	0.9574	0.9494	0.9793	0.9777	0.9995	0.9987
	3	0.9591	0.9539	0.9874	0.9869	0.9988	0.9984
Signs-MNIST	1	0.9507	0.9493	0.9892	0.9853	0.9994	0.9992
	2	0.9418	0.9379	0.9781	0.9769	0.9997	0.9995
	3	0.9699	0.9663	0.9893	0.9851	0.9994	0.9991
Digits-MNIST	1	0.9456	0.9337	0.9866	0.9856	0.9995	0.9977
	2	0.9393	0.9268	0.9837	0.9818	0.9996	0.9993
	3	0.9686	0.9567	0.9899	0.9874	0.9998	0.9995
CIFAR-10	1	0.9431	0.9387	0.9839	0.9821	0.9994	0.9983
	2	0.9496	0.9485	0.9843	0.9813	0.9997	0.9978
	3	0.9686	0.9581	0.9885	0.9881	0.9998	0.9992

Table 6: Best and Average Fitness of Fashion- MNIST, MNIST, Signs- MNIST, Digits-MNIST, and CIFAR-10

Model	Test case	Evaluation	Fashion-MNIST	MNIST	CIFAR-10	Digits-MNIST	Sign-MNIST
GA	1	Accuracy	0.9598	0.9683	0.9517	0.9703	0.9574
		Loss	0.5878	0.4618	0.4419	0.3984	0.5506
	2	Accuracy	0.9483	0.9722	0.9593	0.9662	0.9623
		Loss	0.6372	0.4181	0.4276	0.4386	0.5165
	3	Accuracy	0.9566	0.9769	0.9629	0.9746	0.9689
		Loss	0.5991	0.3671	0.4041	0.3517	0.4871
QIGA1	1	Accuracy	0.9917	0.9816	0.9692	0.9951	0.9792
		Loss	0.1123	0.0924	0.1035	0.0898	0.3233
	2	Accuracy	0.9945	0.9933	0.9753	0.9899	0.9836
		Loss	0.1092	0.0637	0.0837	0.1088	0.0747
	3	Accuracy	0.9972	0.9983	0.9888	0.9988	0.9891
		Loss	0.0608	0.0479	0.0622	0.0387	0.0582
QIGA2	1	Accuracy	0.9929	0.9931	0.9917	0.9883	0.9926
		Loss	0.0583	0.0641	0.0911	0.1274	0.0381
	2	Accuracy	0.9973	0.9994	0.9944	0.9948	0.9998
		Loss	0.0517	0.0396	0.0686	0.0595	0.0202
	3	Accuracy	0.9994	0.9964	0.9996	0.9999	0.9890
		Loss	0.0412	0.0426	0.0206	0.0104	0.1288

Table 7: Accuracy and Loss of Fashion- MNIST, MNIST, Signs- MNIST, Digits-MNIST, and CIFAR-10

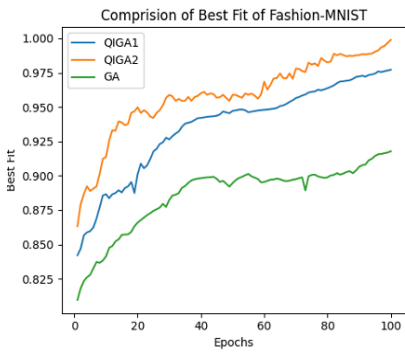


Fig 4: Best-Fit of Fashion-MNIST (Test-1)

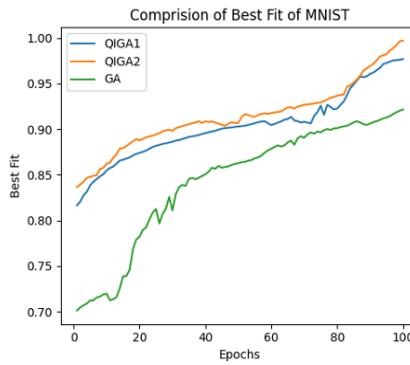


Fig 5: Best-Fit of MNIST (Test-1).

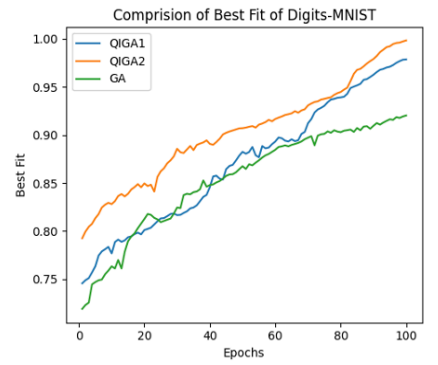


Fig 6: Best-Fit of Digits-MNIST (Test-1)

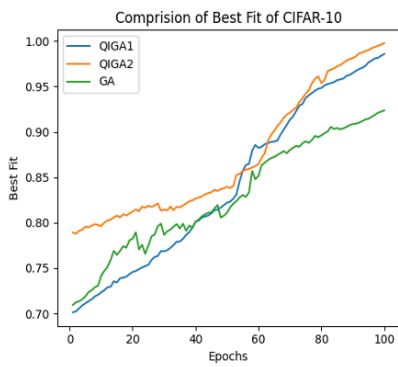


Fig 7: Best-Fit of CIFAR-10 (Test-1).

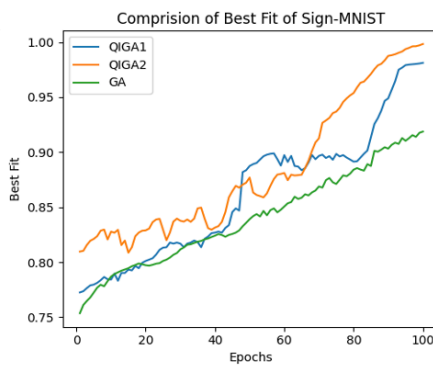


Fig 8: Best-Fit of Sign-MNIST (Test-1)

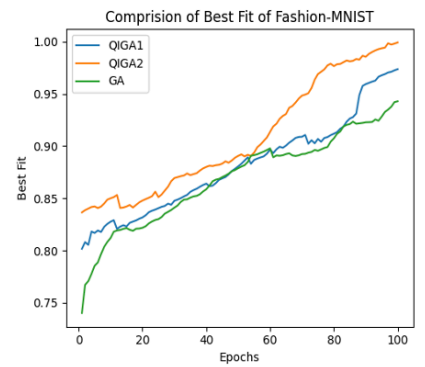


Fig 9: Best-Fit of Fashion-MNIST (Test-2)

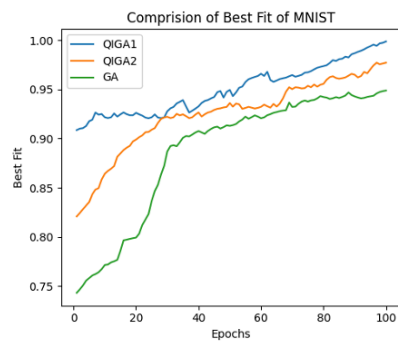


Fig 10: Best-Fit of MNIST (Test-2)

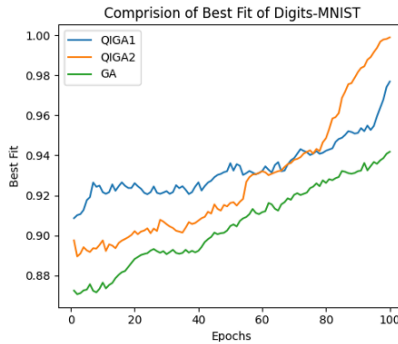


Fig 11: Best-Fit of Digits-MNIST (Test-2)

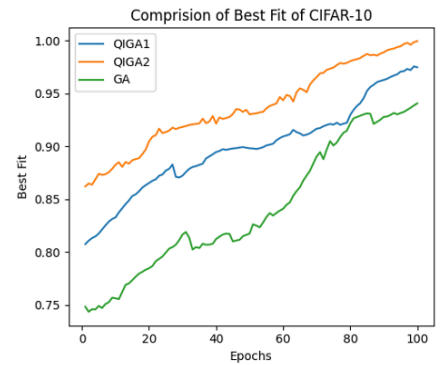


Fig 12: Best-Fit of CIFAR-10 (Test-2)

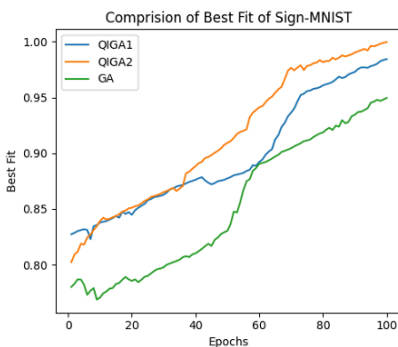


Fig 13: Best-Fit of Sign-MNIST (Test-2)

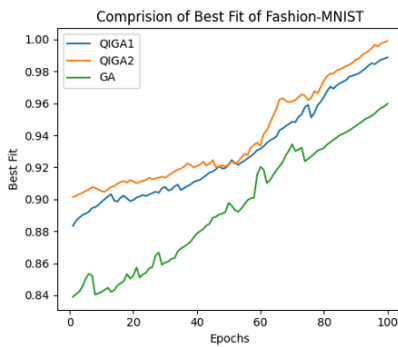


Fig 14: Best-Fit of Fashion-MNIST (Test-3)

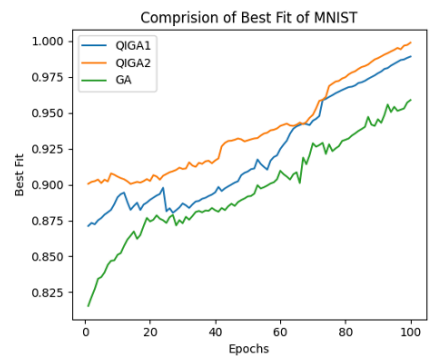


Fig 15: Best-Fit of MNIST (Test-3)

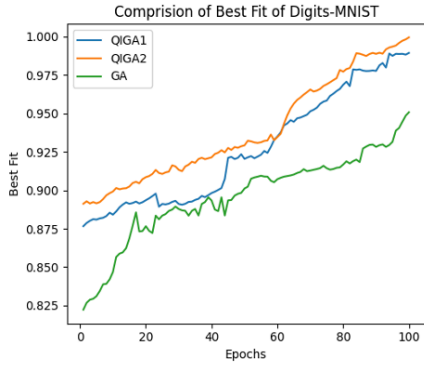


Fig 16: Best-Fit of Digits-MNIST (Test-3)

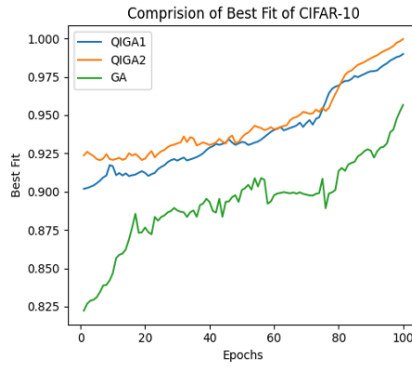


Fig 17: Best-Fit of CIFAR-10 (Test-3).



Fig 18: Best-Fit of Sign-MNIST (Test-3)

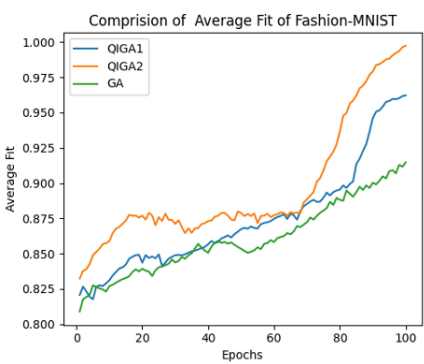


Fig 19: Average -Fit of Fashion-MNIST (Test-1)

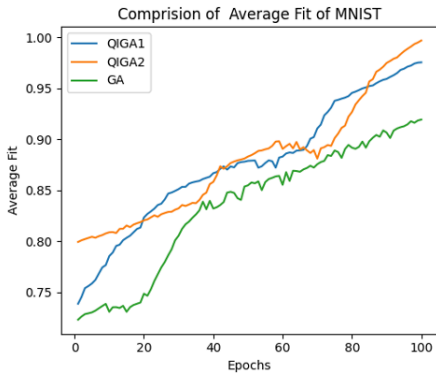


Fig 20: Average -Fit of MNIST (Test-1)

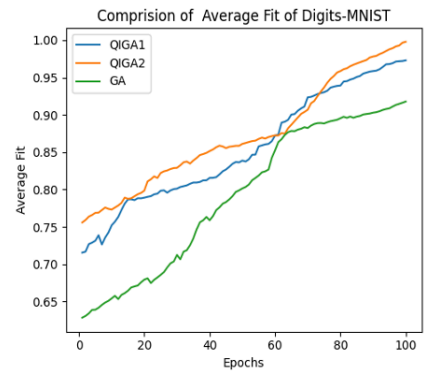


Fig 21: Average-Fit of Digits-MNIST (Test-1)

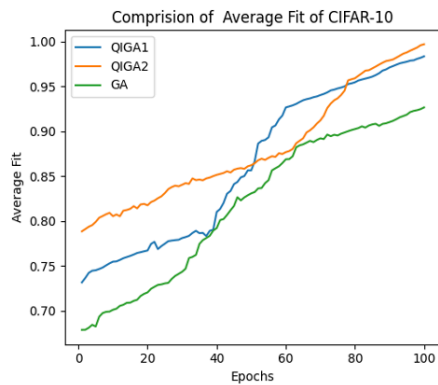


Fig 22: Average -Fit of CIFAR-10 (Test-1)

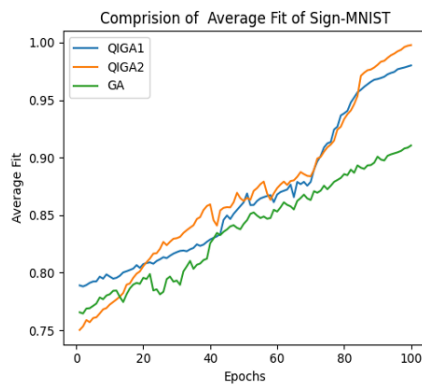


Fig 23: Average-Fit of Sign-MNIST (Test-1).

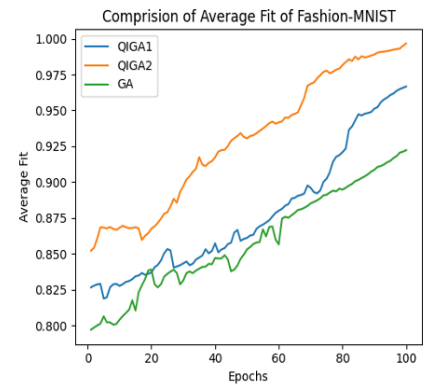


Fig 24: Average-Fit of Fashion-MNIST (Test-2)

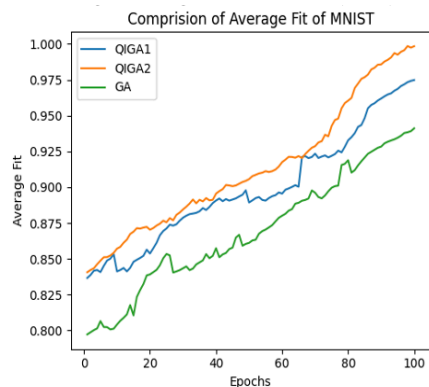


Fig 25: Average -Fit of MNIST (Test-2)

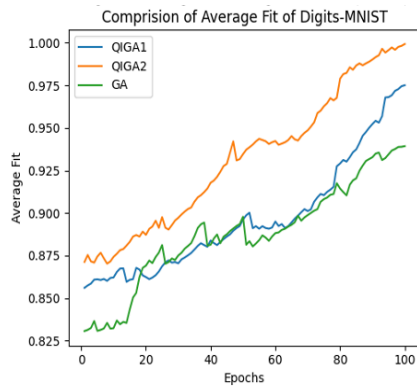


Fig 26: Average-Fit of Digits-MNIST (Test-2)

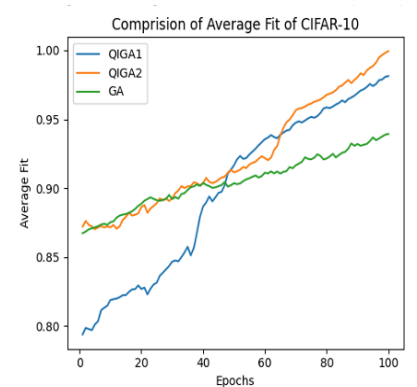


Fig 27: Average-Fit of CIFAR-10 (Test-2)

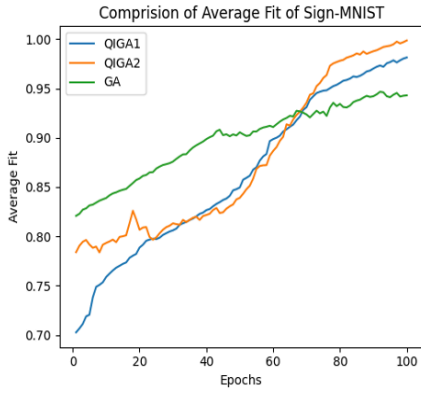


Fig 28: Average-Fit of Sign-MNIST (Test-2)

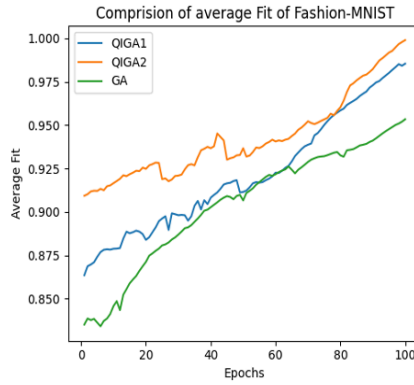


Fig 29: Average-Fit of Fashion-MNIST (Test-3).

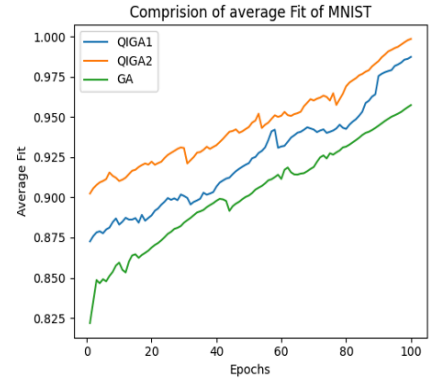


Fig 30: Average-Fit of MNIST (Test-3)

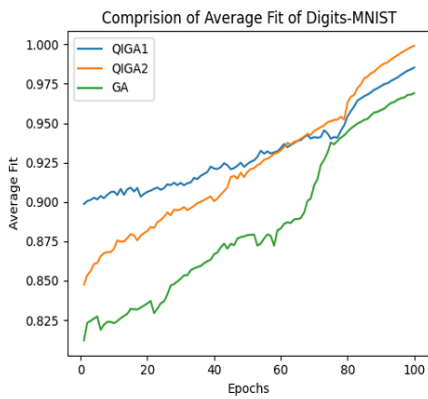


Fig 31: Average-Fit of Digits-MNIST (Test-3)

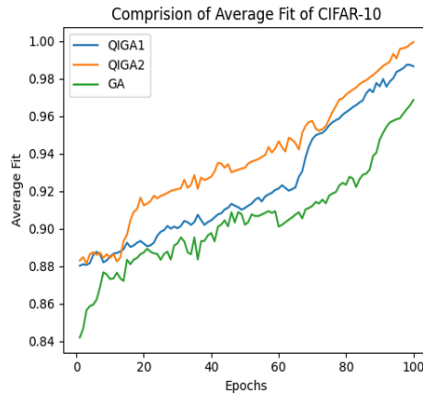


Fig 32: Average -Fit of CIFAR-10 (Test-3)

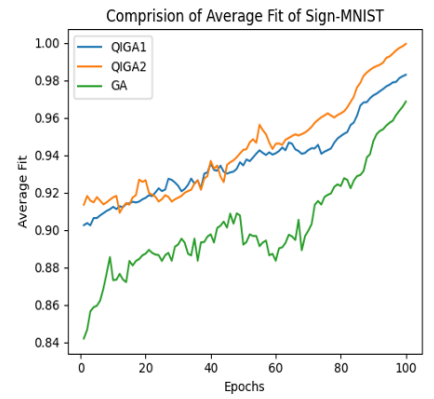


Fig 33: Average-Fit of Sign-MNIST (Test-3)

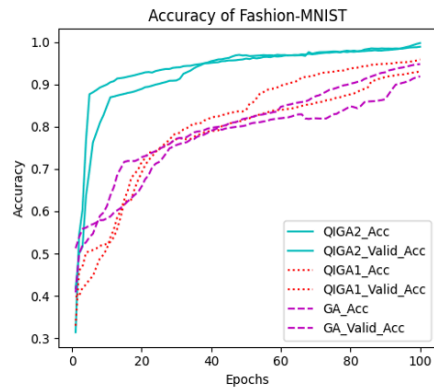


Fig 34: Accuracy of Fashion-MNIST

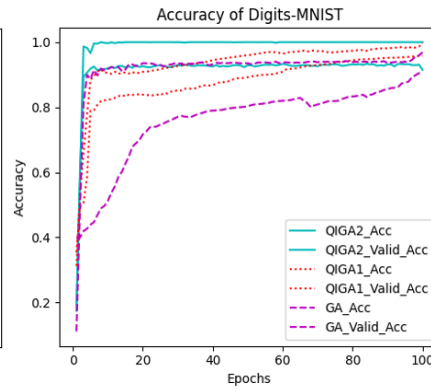


Fig 35: Accuracy of Digits-MNIST

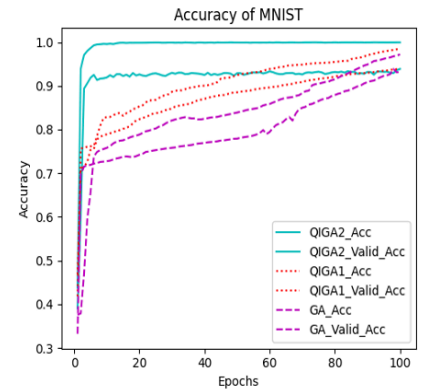


Fig 36: Accuracy of MNIST

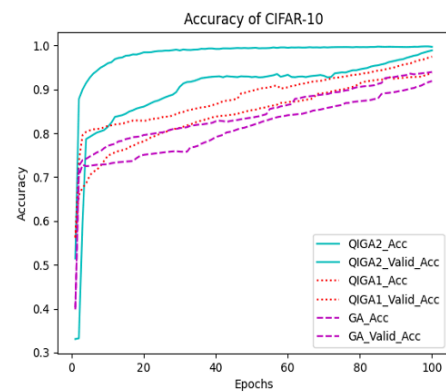


Fig 38: Accuracy of Sign-MNIST

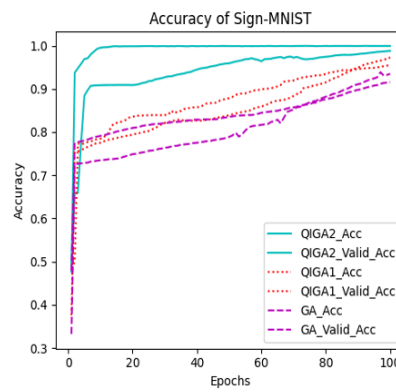


Fig 39: Loss of Fashion-MNIST

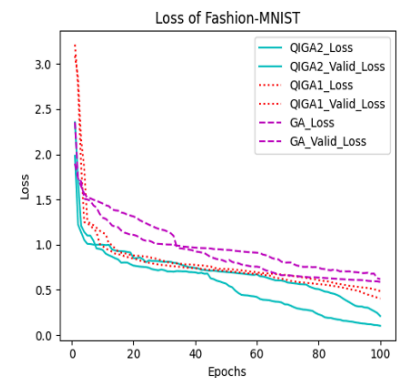


Fig 37: Accuracy of CIFAR-10

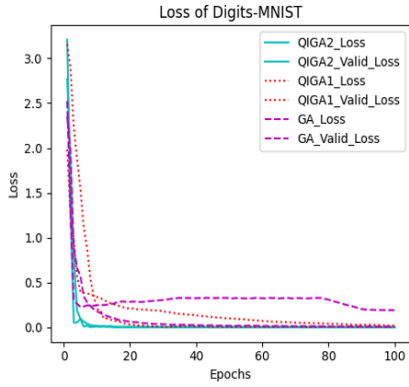


Fig 40: Loss of Digits-MNIST

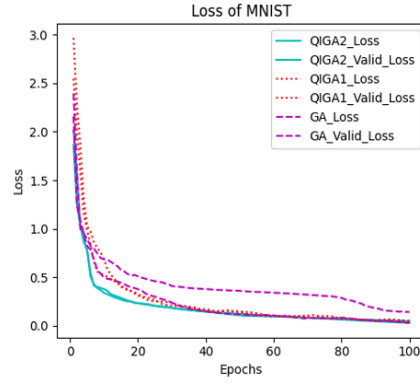


Fig 41: Loss of MNIST

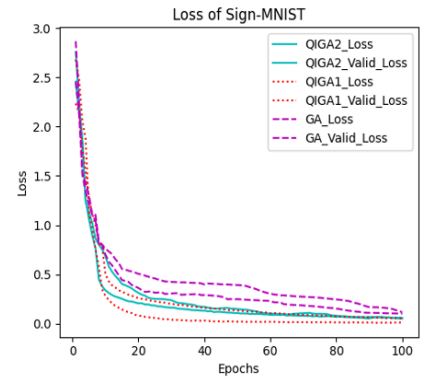


Fig 42: Loss of Sign-MNIST

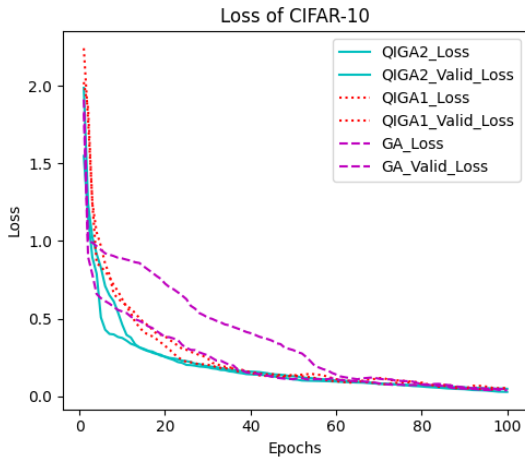


Fig 43: Loss of CIFAR-10

Figure: Fig. 4- Fig. 8 is show Best-Fitness for Test-1, Fig. 9- Fig. 13 is show Best-Fitness for Test-2, Fig. 14- Fig. 18 is show Best-Fitness for Test-3, and Fig. 19- Fig. 23 is show Average-Fitness for Test-1, Fig. 24- Fig. 28 is show Average-Fitness for Test-2, Fig. 29- Fig. 33 is show Average-Fitness for Test-3, and Fig. 34- Fig. 38 is show Accuracy, and Fig. 39- Fig. 43 is show Loss of Fashion-MNIST, MNIST, Sign-MNIST, Digits-MNIST, and CIFAR-10 datasets

5.4.2 Comparative Analysis of Determining Rotating Angle Direction, Mutation, and Crossover Process

Table 6-8 shows the statistical result of 100 generations evolutionary process (GA) and quantum-inspired genetic algorithm (QIGA 1 and 2)) of a given time of optimal, worst, and average of rotation of angle's direction. The genetic process slows down between 40 and 70 generations. Between 60 and 100 generations yields the ideal answer. The x-axis shows the number of epochs; the y-axis shows the best fitness, average fitness, accuracy, and loss of every epoch. The description of the x -axis and the y -axis of the following graphic corresponds with Figures 4-43. Depending on the conventional and quantum genetic process, the rotating angle adaptably changes each epoch. This work investigates three scenarios; the highest and minimum rotation angles of the three cases are correspondingly (a) $(0.001\pi, 0.005\pi)$ (b) $(0.05\pi, 0.08\pi)$ and (c) $(0.001\pi, 0.08\pi)$. All cases use a quantum rotation angle algorithm (algorithm 5) for GA, QIGA 1 and 2. For the three cases, 100 trials were taken; the experimental findings were displayed in Table 8; so, the rotating strategy was chosen for the three cases in this study.

Based on the angle rotation case ((a) $(0.001\pi, 0.005\pi)$ (b) $(0.05\pi, 0.08\pi)$ and (c) $(0.001\pi, 0.08\pi)$) of the QGA, the quantum mutation process is added with a probability of mutation 0.5, 0.6, and 0.8. By running the quantum mutation algorithm (algorithm 8) 100 times, Table 8 presents the experiment's statistical (optimal, worst, and average time) findings for GA, QIGA (1 and 2). We can thus conclude once more that the speed of development is enhanced. Applying the quantum mutation method in five MNIST datasets allows us to get the optimal solution with 100 generations. Once more, the speed of evolution is enhanced; convergence times likewise increase.

The quantum crossover process is incorporated with a probability of mutation 0.2, 0.4, and 0.6 based on the angle rotation case ((a) $(0.001\pi, 0.005\pi)$ (b) $(0.05\pi, 0.08\pi)$ and (c) $(0.001\pi, 0.08\pi)$) and quantum mutation 0.5, 0.6, and 0.8 of the QGA. Table 8 shows the experiment's statistical results (optimal, worst, and average time) by performing the quantum crossover method (algorithm 7) 100 times for GA, QIGA (1 and 2). Once more, the development speed is improved; convergence times also increase. Please note that experiments may vary in hardware configuration and internet speed for dataset training and feature extraction processes.

Test Case	Rotating Angle Strategy	Model	Rotation Strategy			Mutation in QGA			Crossover in QGA		
			Optimal	worst	Average	Optimal	worst	Average	Optimal	worst	Average
1	(a)	GA	25.7601	28.6613	26.7345	25.9988	29.2387	26.9979	26.5643	29.8112	27.0267
		QIGA1	14.6776	18.7093	15.4712	15.4327	18.9907	15.7868	15.9896	19.2355	16.3423
		QIGA2	12.5478	16.5907	13.7345	12.8601	16.9021	13.9911	13.2345	17.3659	13.9125
	(b)	GA	14.8522	15.8691	14.8566	15.2379	16.2148	15.8769	15.8124	16.6102	16.2768
		QIGA1	9.4286	10.9327	9.7136	9.9843	11.5453	10.6965	10.9666	12.8521	11.0011
		QIGA2	8.4533	9.8565	8.7021	8.5783	10.0066	8.9672	9.2432	10.8995	9.7756
	(c)	GA	22.7589	25.7742	23.0684	23.0453	26.1482	23.8461	24.0122	26.7333	24.8726
		QIGA1	17.9264	19.9664	17.9895	18.1234	20.6523	18.3897	18.7392	22.2351	19.0326
		QIGA2	13.7369	14.7521	13.9682	14.2439	15.9859	14.6999	15.1218	16.1122	15.9001
2	(a)	GA	19.5843	21.9678	19.9579	19.7528	21.8839	19.9977	20.9893	23.9872	21.5864
		QIGA1	12.8947	13.8672	12.9981	12.8982	13.9695	13.1127	13.7866	15.3587	13.9925
		QIGA2	9.9678	10.9911	10.1581	10.8276	12.0163	11.0062	11.7114	12.8427	12.1735
	(b)	GA	14.8525	15.9468	14.8599	14.6763	16.1932	14.9864	15.9869	16.7488	15.9736
		QIGA1	9.7165	10.8945	10.1143	9.9816	11.0745	10.2192	9.9988	10.9893	10.1534
		QIGA2	5.9437	6.8773	6.1875	6.1986	7.5188	6.4971	7.1834	8.2474	7.5147
	(c)	GA	21.7491	23.6745	22.0444	22.8256	24.3795	23.0376	23.7631	25.9867	23.8943
		QIGA1	19.9854	20.9682	20.2259	20.4127	21.7886	20.6991	21.3897	22.8934	21.9275
		QIGA2	8.9783	9.9674	9.1372	9.8945	10.8679	9.4765	9.8948	11.9271	10.3791
3	(a)	GA	20.9874	22.8962	21.7856	21.9873	23.9856	22.0898	22.7815	24.8279	23.0862
		QIGA1	10.6843	11.8875	10.3654	10.8862	11.9327	11.0131	11.9986	12.7892	12.0163
		QIGA2	8.4691	9.8892	8.9145	8.9333	10.2537	9.3569	9.9054	10.9863	10.1212
	(b)	GA	22.6291	23.8673	22.9852	23.4798	25.9539	23.8987	23.9895	26.9199	24.6874
		QIGA1	10.7877	11.8334	11.0302	10.9012	12.0618	11.1788	11.8951	12.9989	12.1792
		QIGA2	7.8976	8.8218	8.0347	7.6971	8.5629	7.9682	8.3743	9.9754	8.8669
	(c)	GA	20.5633	21.9487	20.8722	21.8986	23.0843	22.0761	23.1985	25.1493	23.5856
		QIGA1	14.6937	15.9891	14.9031	14.3237	15.3869	14.8792	15.8796	16.7929	16.2143
		QIGA2	9.5489	10.5867	9.9785	9.8955	10.8788	10.1043	10.9984	12.4867	11.8779

Table 8: Optimal, Worst, and Average time (s) of direction rotation of angle, mutation, and crossover for MNIST-Datasets

5.5 Complexity Analysis

The worst-case scenario time complexity analysis of our proposed model QIGA is defined in the steps below.

1. In the QIGA model, Worst Time Complexity ($T_{Complex}$) is used to prepare the initialization of chromosomes with population size P and individual length Ind_{Length} . (where length Ind_{Length} is measured by maximum intensity of image as $Ind_{Length} = Int_{img} \times Int_{img}$.) is $O(P \times Ind_{Length})$ or $O(P \times Int_{img} \times Int_{img})$.
2. In the next step, each chromosome is prepared with quantum state population matrix Q concerning P , and $T_{Complex}$ is $O(P \times Ind_{Length})$.
3. Evaluate threshold value with specific parameters (probability parameters) and capacity, then $T_{Complex}$ is $O(P \times Ind_{Length})$.
4. The $T_{Complex}$ of measure feature selection and extraction (quality) of the image with quantum encoded of each pixel (image) is $O(P \times Ind_{Length})$.
5. The $T_{Complex}$ evaluates the fitness of each chromosome is $O(P)$.
6. The $T_{Complex}$ of the quantum rotation gate process used on the quantum population to give a new quantum state with the best chromosome is $O(P \times Ind_{Length})$.
7. The $T_{Complex}$ of the quantum selection process, quantum mutation, and quantum crossover is $O(P \times Ind_{Length})$.
8. The overall time complexity ($T_{Complex}$) of our proposed model QIGA is $O(P \times Ind_{Length} \times Iteration_{max})$.

5.6 Comparative Analysis- Combining GA with Quantum-based feature selection and extraction with a dynamic approach improved classification accuracy ratios for Fashion-MNIST, MNIST, Sign-MNIST, Digits-MNIST, and CIFAR-10 using 100 epochs of experimentation. QIGA, with 100 epochs, produced the most accurate categorization results. Table 7 shows how the suggested approach can accurately classify all five databases. We compared our proposed model with other author's models and show the comparison in Table 9 below.

Reference	Used Datasets	Used Approach	Complexity Analysis	Accuracy (%)
W. Ye et al., 2020	MNIST	QIEA	No	98.97
Andrés et al., 2023	MNIST	FCNN and QCNN	No	98
Y. Sun et al., 2020	CIFAR-10	CNN-GA	No	96.78
Liu et al., 2023	CIFAR100, CIFAR10, Fashion, MRB,	Leader-Follower Evolution Mechanism with Multi-Object	No	98.07

	MRI MRDBI, MB, and MRD.	Genetic Programming (LF-MOGP)		
Li et al., 2023	MNIST	Evolutionary Quantum Neural Architecture	No	98.99
Proposed Model	Fashion-MNIST	QIGA-based Feature Selection and Extraction (QIGA1) and QIGA-based Feature Selection and Extraction with Dynamic approach and QIGA2)	Yes	99.72 and 99.94
	MNIST			99.83 and 99.94
	Sign-MNIST			98.91 and 99.98
	Digits-MNIST			99.88 and 99.99
	CIFAR-10			98.88 and 99.96

Table 9: Comparison of proposed model with other models

5.7 Conclusion

In this study, we introduce two novel quantum-inspired meta-heuristic algorithms, precisely the quantum-inspired genetic algorithm (QIGA1) with filter- feature selection extraction based GA and the QIGA with a dynamic approach (QIGA2), tailored for benchmark datasets such as Fashion-MNIST, MNIST, and Digits-MNIST, Signs-MNIST, and CIFAR-10 thresholding. These algorithms use various measures to determine optimal threshold values for grayscale test images. In the proposed algorithms, the participating gens or chromosomes undergo a random selection of quantum interference process, and there is no need for prior lookup tables to facilitate this interference. The effectiveness of these proposed methods has been assessed by comparing them to their traditional counterparts (GA) and subsequently with the QIGA. In order to address the challenges posed by high-dimensional and grayscale test benchmark datasets, this paper proposed a dynamic strategy combining filter feature selection techniques and a QGA for feature extraction and selection. During the initial phase of the suggested dynamic filter-genetic feature selection approach, the top 10% of features identified by gain ratio and gain information are chosen, while extraneous and irrelevant features are discarded to alleviate the issues associated with high dimensionality and grayscale test multiarray datasets. The reduced datasets containing only the highest-ranked features from the filter methods undergo further optimization through QGA to enhance classification outcomes for the MNIST dataset. The experimental results indicated that the QIGA in the proposed methods eliminated nearly 50% of irrelevant features from the MNIST datasets, which had been reduced by filter methods in the preliminary step, thus ensuring that only the crucial features were utilized to optimize the MNIST dataset classification performance of the classifiers. Moreover, the dynamic filter-QGA feature selection methods exhibited significantly improved performance compared to the standalone classifiers or their performance when only filter algorithms were employed. The dynamic filter-QGA method also surpassed other feature selection techniques on most high-dimensional and grayscale test multiarray datasets analysed in this research. The findings indicate that Quantum-inspired meta-heuristic algorithms (QIGA 1 and 2) are more precise and robust than traditional meta-heuristic algorithms (GA), although there are a few exceptions. The QIGA method proved to be the most efficient in terms of computational time. Therefore, employing a quantum mechanism reduces time complexity relative to traditional algorithms, suggesting promising directions for future research.

CRediT authorship contribution statement

Akhilesh Kumar Singh: Writing – review & editing, Writing – original draft, Visualization, Validation, Software, Resources, Methodology, Investigation, Formal analysis, Data curation, Conceptualization.

Kirankumar R. Hiremath: Review & editing, Validation, Supervision.

Conflict Of Interest

Authors declare no conflict of interest

Data Availability Statement

Data will be made available on request.

References

[1] A. Narayanan and M. Moore (1996). Quantum-inspired genetic algorithms. In proceedings of the IEEE International Conference on Evolutionary Computation (ICEC '96), pp. 61–66, Nagoya, Japan. doi: 10.1109/ICEC.1996.542334.

[2] Arsenii Senokosov, Alexandr Sedykh, Asel Sagingalieva, Basil Kyriacou and Alexey Melnikov (2024). Quantum machine learning for image classification. Machine Learning Science and Technology, Vol. 5 (1) 015040. doi: <https://doi.org/10.1088/2632-2153/ad2aef>

[3] Ali Mohsen, Mo Tiwari (2021). Image Compression and Classification Using Qubits and Quantum Deep Learning. doi: <https://doi.org/10.48550/arXiv.2110.05476>

[4] Alisson Steffens Henrique, Anita Maria da Rocha Fernandes, Rodrigo Lyra, Valderi Reis Quietinho Leithardt, Sérgio D. Correia, Paul Crocker, Rudimar Luis Scaranto Dazzi (2021). Classifying Garments from Fashion-MNIST Dataset Through CNNs. Advances in Science, Technology and Engineering Systems Journal, Vol. 6, No. 1, pp. 989-994. doi: 10.25046/aj0601109

[5] Andr es Felipe Guerrero Gonz alez, Leonardo Florez Valencia (2023). Classical-quantum convolutional networks for image classification. Journal Of IEEE Transactions On Artificial Intelligence.

doi:https://repository.javeriana.edu.co/bitstream/handle/10554/65492/attachment_0_Masters_Thesis-%281%29.pdf?sequence=1&isAllowed=y (Activated on Jan, 2025)

[6] Il-Hyang Choe, Gwang-Jin Kim, Nam-Chol Kim, Myong-Chol Ko, Ju-Song Ryom, Ryong-Min Han, Tae-Gyong Han & Il Han (2023). Can quantum genetic algorithm really improve quantum backpropagation neural network?. Quantum Inf Process 22, 154. doi:<https://doi.org/10.1007/s11128-023-03858-w>

[7] Creevey, F.M., Hill, C.D. & Hollenberg, L.C.L. (2023). GASP: a genetic algorithm for state preparation on quantum computers. Sci Rep 13, 11956. doi:<https://doi.org/10.1038/s41598-023-37767-w>

- [8] F. Shi, H. Wang, L. Yu, and F. Hu (2010). Analyze of 30 Cases of MAT-LAB Intelligent Algorithms, Beihang University Press, Beijing, China.
- [9] Iordanis Kerenidis, Alessandro Luongo (2020). Quantum Classification of the MNIST Dataset with Slow Feature Analysis. *Phys. Rev. A* 101, 062327. doi: <https://doi.org/10.1103/PhysRevA.101.062327>
- [10] J. G. Proakis (2000). *Digital Communications*. Mc Graw-Hill, New York, NY, USA, 4th Edition.
- [11] J. Huang, R. A. Berry, and M. L. Honig (2006). Auction-based spectrum sharing. *Mobile Networks and Applications*, vol. 11, no. 3, pp. 405–418. doi: <http://dx.doi.org/10.1007/s11036-006-5192-y>
- [12] J. Zhang, H. Li, Z. Tang, Q. Lu, X. Zheng, and J. Zhou (2014). An improved quantum-inspired genetic algorithm for image multilevel thresholding segmentation. *Math. Problems in Eng*, pp. 1–12. doi: <https://doi.org/10.1155/2014/295402>
- [13] K. H. Han and J. H. Kim (2000). Genetic quantum algorithm and its application to combinatorial optimization problem. in *Proceedings of the Congress on Evolutionary Computation*, pp. 1354–1360. doi: https://www.researchgate.net/publication/2573070_Genetic_Quantum_Algorithm_and_its_Application_to_Combinatorial_Optimization_Problem
- [14] K. H. Han and J. H. Kim (2002). Quantum-Inspired Evolutionary Algorithm for a Class of Combinatorial Optimization. *IEEE Transactions on Evolutionary Computation*, vol. 6, no. 6, pp. 580–593. doi: <http://dx.doi.org/10.1109/TEVC.2002.804320>
- [15] Kevin Shen, Bernhard Jobst, Elvira Shishenina, Frank Pollmann (2024). Classification of the Fashion-MNIST Dataset on a Quantum Computer. doi: <https://doi.org/10.48550/arXiv.2403.02405>
- [16] Lentzas, A.; Nalmpantis, C.; Vrakas, D. (2019). Hyperparameter Tuning using Quantum Genetic Algorithms. In *Proceedings of the 2019 IEEE 31st International Conference on Tools with Artificial Intelligence (ICTAI)*, Portland, OR, USA, pp. 412–416. doi: [10.1109/ICTAI.2019.00199](https://doi.org/10.1109/ICTAI.2019.00199)
- [17] Qingqing Liu, Xianpeng Wang, Yao Wang, Xiangman Song (2023). Evolutionary convolutional neural network for image classification-based on multi-objective genetic programming with leader–follower mechanism. *Complex & Intelligent Systems*, Vol. 9, pp. 3211–3228. doi: <https://doi.org/10.1007/s40747-022-00919-y>
- [18] Phalak, K., Ghosh, A., & Ghosh, S (2024). Optimizing Quantum Embedding using Genetic Algorithm for QML Applications. doi: <https://doi.org/10.48550/arXiv.2412.00286>
- [19] Ranga, D.; Prajapat, S.; Akhtar, Z.; Kumar, P.; Vasilakos, A.V. (2024). Hybrid Quantum–Classical Neural Networks for Efficient MNIST Binary Image Classification. *Mathematics* 12, 3684. doi: <https://doi.org/10.3390/math12233684>

- [20] Riaz, F., Abdulla, S., Suzuki, H., Ganguly, S., Deo, R. C., & Hopkins, S (2023). Accurate Image Multi-Class Classification Neural Network Model with Quantum Entanglement Approach. *Sensors*, 23(5), 2753. doi: <https://doi.org/10.3390/s23052753>
- [21] R. Lahoz-Beltra (2016). Quantum Genetic Algorithms for Computer Scientists. *Computers*, vol. 5, no. 4, p. 24. doi: <https://doi.org/10.3390/computers5040024>
- [22] Rui Shao, Gong Zhang, Xiao Gong (2022). Generalized robust training scheme using genetic algorithm for optical neural networks with imprecise components. *Photonics Research*, Vol. 10, No. 8, pp. 1868-1876. doi: <https://doi.org/10.1364/PRJ.449570>
- [23] S. Y. Yang, F. Liu, and L. C. Jiao (2004). Novel genetic algorithm based on the quantum chromosome. *Journal of Xidian University*, vol. 31, no. 1, pp. 76–81. doi: <https://journal.xidian.edu.cn/xdxj/EN/Y2004/V31/I1/76>
- [24] S. Zhou, W. Pan, B. Luo, W. L. Zhang, and Y. Ding (2006). A novel quantum genetic algorithm based on particle swarm optimization method and its application. *Acta Electronica Sinica*, vol. 34, no. 5, pp. 897–901. doi: <https://www.ejournal.org.cn/EN/Y2006/V34/I5/897>
- [25] Sophie Choe (2022). Continuous Variable Quantum MNIST Classifiers. doi: <https://doi.org/10.48550/arXiv.2204.01194>
- [26] Soumyadip Sarkar (2024). Quantum Transfer Learning for MNIST Classification Using a Hybrid Quantum-Classical Approach. doi: <https://doi.org/10.48550/arXiv.2408.03351>
- [27] W. Ye, R. Liu, Y. Li and L. Jiao (2020). Quantum-Inspired Evolutionary Algorithm for Convolutional Neural Networks Architecture Search. *IEEE Congress on Evolutionary Computation (CEC)*, Glasgow, UK, pp. 1-8, doi: 10.1109/CEC48606.2020.9185727.
- [28] Y. Sun, B. Xue, M. Zhang, G. G. Yen and J. Lv (2020). Automatically Designing CNN Architectures Using the Genetic Algorithm for Image Classification. in *IEEE Transactions on Cybernetics*, vol. 50, no. 9, pp. 3840-3854. doi: 10.1109/TCYB.2020.2983860.
- [29] Yangyang Li, Ruijiao Liu, Xiaobin Hao, Ronghua Shang, Peixiang Zhao, Licheng Jiao (2023). EQNAS: Evolutionary Quantum Neural Architecture Search for Image Classification. *Neural Networks* Vol. 168, pp. 471–483. doi: <https://doi.org/10.1016/j.neunet.2023.09.040>
- [30] Yakoub Bazi, Lorenzo Bruzzone, Farid Melgani (2007). Image thresholding based on the EM algorithm and the generalized Gaussian distribution. *Pattern Recognition* Vol. 40, pp 619–634. doi: <https://doi.org/10.1016/j.patcog.2006.05.006>